

Formation of natural gas hydrates in marine sediments

1. Conceptual model of gas hydrate growth conditioned by host sediment properties

M. Ben Clennell,^{1,2} Martin Hovland,³ James S. Booth,⁴
Pierre Henry,⁵ and William J. Winters⁴

Abstract. The stability of submarine gas hydrates is largely dictated by pressure and temperature, gas composition, and pore water salinity. However, the physical properties and surface chemistry of deep marine sediments may also affect the thermodynamic state, growth kinetics, spatial distributions, and growth forms of clathrates. Our conceptual model presumes that gas hydrate behaves in a way analogous to ice in a freezing soil. Hydrate growth is inhibited within fine-grained sediments by a combination of reduced pore water activity in the vicinity of hydrophilic mineral surfaces, and the excess internal energy of small crystals confined in pores. The excess energy can be thought of as a “capillary pressure” in the hydrate crystal, related to the pore size distribution and the state of stress in the sediment framework. The base of gas hydrate stability in a sequence of fine sediments is predicted by our model to occur at a lower temperature (nearer to the seabed) than would be calculated from bulk thermodynamic equilibrium. Capillary effects or a build up of salt in the system can expand the phase boundary between hydrate and free gas into a divariant field extending over a finite depth range dictated by total methane content and pore-size distribution. Hysteresis between the temperatures of crystallization and dissociation of the clathrate is also predicted. Growth forms commonly observed in hydrate samples recovered from marine sediments (nodules, and lenses in muds; cements in sands) can largely be explained by capillary effects, but kinetics of nucleation and growth are also important. The formation of concentrated gas hydrates in a partially closed system with respect to material transport, or where gas can flush through the system, may lead to water depletion in the host sediment. This “freeze-drying” may be detectable through physical changes to the sediment (low water content and overconsolidation) and/or chemical anomalies in the pore waters and metastable presence of free gas within the normal zone of hydrate stability.

1. Introduction

Current models for the formation and distribution of gas hydrates in marine sediments generally assume that the phase equilibria of a bulk water and gas mixture (Figure 1) measured under laboratory conditions [Dholabhai *et al.*, 1991; Dickens and Quinby-Hunt, 1997] can be applied directly to the natural environment [Kvenvolden, 1993; Dillon *et al.*, 1993; Paull *et al.*, 1994]. (By bulk we mean a body of material of sufficient size that local fluctuations in properties average out, and surface energy terms are small compared with other contributions to free energy.) However, laboratory tests do not cover the range of pressures found in nature and bulk pressure-vessel experiments do not account for effects of host-sediment properties on hydrate stability. According to Hyndman *et al.* [1992, p. 292] “...the role of clay surface activity and the fine pore spaces in deep sea sediments is unknown.”

Gas hydrates recovered from beneath the seafloor display a wide range of growth habits and tend to be patchily distributed within the host sediment according to texture [Ginsburg *et al.*, 1993; Ginsburg and Soloviev, 1994, 1997; Booth *et al.*, 1996]. While the base of hydrate stability in the marine subsurface has often been found at the approximate conditions of pressure and temperature given by bulk phase equilibria [Hyndman *et al.*, 1992; Tréhu *et al.*, 1995], there are a number of ocean drilling sites where the depth range over which hydrates occur is narrower than that predicted [Westbrook *et al.*, 1994; Paull *et al.*, 1997]. The sediment somehow inhibits gas hydrate nucleation and growth, an inference supported by experimental data on gas hydrate formation in porous media [e.g., Makogon, 1981; Yousif and Sloan, 1991; Handa and Stupin, 1992; Melnikov and Nesterov, 1996]. Here we review the evidence for host-sediment effects on the stability and growth habits of gas hydrates and propose some explanations.

Ginsburg [1998] distinguishes two categories of submarine gas hydrates: those which occur throughout the sediment often extending down to the base of hydrate stability (deep seated), and local, concentrated accumulations associated with focused gas flow features such as mud volcanoes (seepage related). While we can make some inferences about thermodynamic stability from hydrates that lie close to the phase boundary, the shallower manifestations tell us that gas can move up through sediments without necessarily combining with water to form clathrates. It is important to view natural gas hydrates in this perspective. There is a particular set of conditions controlling equilibrium

¹ Department of Earth Sciences, University of Leeds, England.

² Now at Centro de Pesquisa em Geofísica e Geologia, Universidade Federal da Bahia, Salvador, Brazil.

³ Statoil, N-4035, Stavanger, Norway.

⁴ United States Geological Survey, Woods Hole, Massachusetts.

⁵ Laboratoire de Géologie, Ecole Normale Supérieure, Paris.

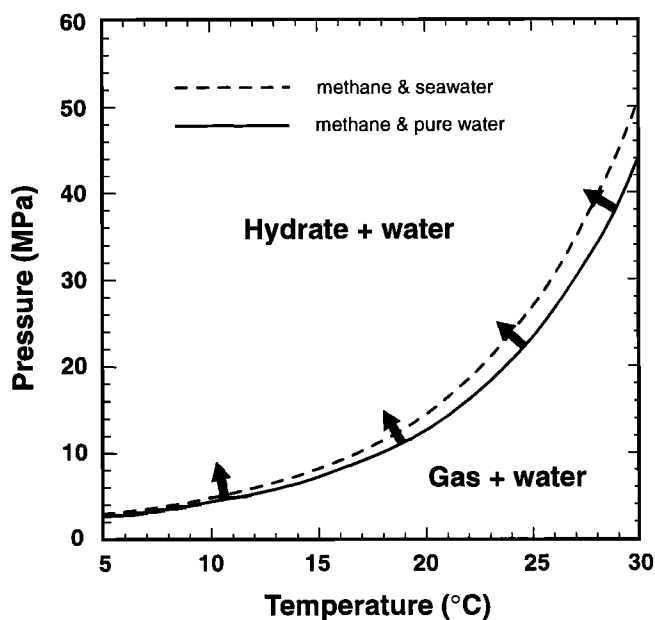


Figure 1. Simplified phase diagram showing the stability field of pressure and temperature for gas hydrates under conditions found in the marine subsurface assuming pure methane gas and seawater fluid composition. Solid arrows indicate the displacement of the phase boundary line to higher pressure and/or lower temperature if gas hydrate is inhibited by some mechanism.

thermodynamic stability in a certain sediment at any depth, but a general model must also allow for possible disequilibrium arising from limitations of reactant supply and transport, and the kinetics in nucleation and growth of gas bubbles and hydrate crystals. Here we examine the quasistatic equilibrium between phases, and we make qualitative predictions about the system behavior through time. Our approach is complementary to porous-continuum models [Rempel and Buffett, 1997, 1998; Xu and Ruppel, 1999], which quantify the dynamic equilibrium that evolves when fluxes of methane, water and heat pass through the sediment column.

Since the structure of natural gas hydrates is similar to that of water ice [Sloan, 1990], we develop the analogy between the formation of natural hydrates and the processes that occur during freezing in porous media and in permafrost in soils. A number of authors [e.g., Trofimuk *et al.*, 1972; Pearson, 1981; Ershov *et al.*, 1993] have already noted that segregated forms of gas hydrate in fine sediments closely resemble ice lenses that grow in fine-grained soils, while in coarser sediment, hydrates grow within the pores and cement the grains strongly together so that loose sand becomes "frozen solid" with commensurate changes in physical properties [Pearson *et al.*, 1983]. MacDonald *et al.* [1994] document gas hydrate outcrops on the seafloor of the Gulf of Mexico that are similar in size and appearance to permafrost ice lenses.

There are important differences between hydrates and permafrost ice. We need to take into account the presence of a gas phase (dominantly methane), which, unlike air in soil, participates in the formation of the crystalline solid. The availability of methane may limit the hydrate-forming reaction, but we will also describe circumstances where water limitation drives the dynamics of the system. Ice lens formation and frost heave take

place under strong thermal gradients within the soil (several degrees Celsius per meter), with the thermodynamic drive for the transport of water to the point of crystal growth coming from undercooling of the water below the normal freezing point within the sediment pores [Konrad and Duquenois, 1993]. The temperature gradients in deep ocean sediments are typically $0.02\text{--}0.08\text{ }^{\circ}\text{C m}^{-1}$ so that another thermodynamic drive, namely, supersaturation due to an excess of methane or undercooling below the normal equilibrium temperature, is needed to produce concentrated accumulations of gas hydrates. Nevertheless, the thermodynamics underlying freezing in porous solids, as described by the capillary-ice model of Everett [1961], provide a good starting point for the analysis of gas hydrate formation in sediments.

Following some observational and theoretical background, we describe a model of gas hydrate stability based largely on principles from soil physics. In a companion paper, Henry *et al.* [this issue] develop our conceptual model to make quantitative predictions of gas hydrate stability, and these are tested against observations of gas hydrate occurrence at the Blake Ridge from Ocean Drilling Program Leg 164 [Paull *et al.*, 1997].

2. Bottom Simulating Reflectors and the Gas Hydrate Phase Boundary

The inferred base of gas hydrate stability beneath the sea floor is often marked by a seismic reflector with negative impedance contrast [Stoll *et al.*, 1971; Shipley *et al.*, 1979]. Given that gas and fluid composition change little with depth, and that the fluid pressure profile is very close to hydrostatic [Hyndman *et al.*, 1992], the reflector can be taken to represent a univariant phase boundary that is nearly isothermal and roughly parallels the seafloor. Accordingly, it is known as the bottom-simulating reflector (BSR).

There is some dispute as to the physicochemical regime that produces the BSR [Brown *et al.*, 1996]. Hyndman and Davis [1992] and Hyndman and Spence [1992] suggested that the reflection arose at the boundary between a hydrate-bearing layer with high-velocity overlying sediments with a normal velocity. In several localities it has been shown that the BSR more likely marks a boundary between overlying sediments containing a little hydrate and an underlying low-velocity zone, typically a few meters to many tens of meters thick, in which there is a small proportion of free gas in the pore space [Miller *et al.*, 1991; MacKay *et al.*, 1994; Singh *et al.*, 1993; Andreassen *et al.*, 1995; Hovland *et al.*, 1997]. The latter situation is shown in Figure 2. Below the depth of intersection between the geotherm and the phase boundary, methane in excess of aqueous solubility will be present as a free gas phase (bubbles in the sediment). Between this depth and the seafloor, hydrate will fill some proportion of the sediment pores providing there is enough gas available to stabilize the clathrate structure.

The primary indicator of gas hydrate stability conditions is the position of the BSR, as existing models would predict that gas first appears at the depth limit of hydrate stability, that is, the thermodynamic three-phase equilibrium. The P,T conditions of the phase boundary can be deduced from measurements of the thermal gradient and the total depth to the BSR beneath sea level. This locus of pressure and temperature can be compared with the gas hydrate stability curve calculated or measured in the laboratory for the particular gas and fluid compositions prevailing. If the BSR should be at a higher, cooler position in the

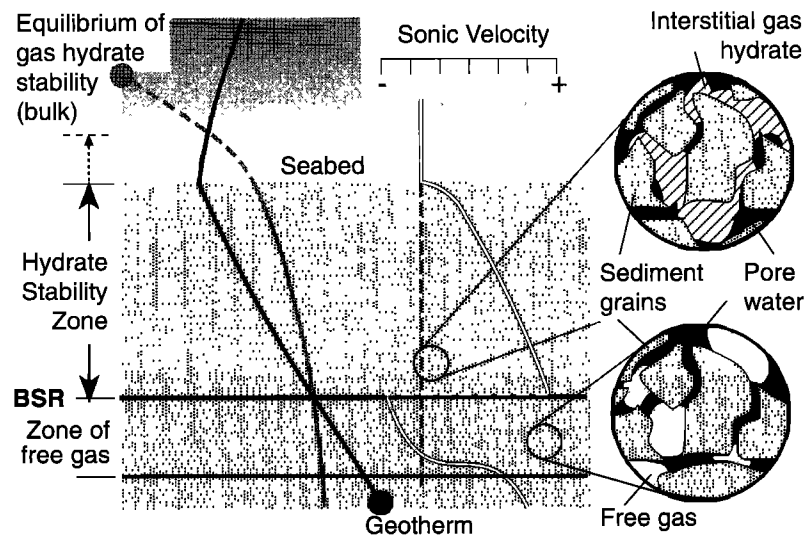


Figure 2. Conventional model for gas hydrate stability and bottom-simulating reflectors in submarine sediments. The base of hydrate stability is marked by a univariant phase boundary as temperature increases deeper into the sediment. At this point methane in excess of solubility in water may exist as free gas and potentially produce a distinct seismic reflector due to reduced velocity.

sediment column than the predicted phase boundary, then we can deduce that either some mechanism is inhibiting gas hydrate stability or the system is out of thermal, hydrostatic, or chemical equilibrium. On the other hand, to explain a BSR that lies deeper than expected (warmer conditions) either requires some mechanism that promotes hydrate stability or a dynamic mechanism preventing attainment of thermodynamic equilibrium.

One mechanism of inhibition that has been quantified is the depression of water activity due to the presence of salts [Dickens and Quinby-Hunt, 1997]. Seawater (which is composed of many salts but depresses water activity to approximately the same degree as a 1 M NaCl solution), typically reduces the equilibrium temperature of the pure methane + pure water phase boundary by 1-2°C. Methane hydrate stability is promoted very strongly by the presence of even small amounts of ethane, carbon dioxide, hydrogen sulfide, and higher hydrocarbons. For example, 1% ethane would approximately counterbalance the effect of the seawater inhibition. These shifts of a few degrees Celsius, would at normal thermal gradients correspond to a change in the position of the BSR of tens of meters. Several disequilibrium effects could produce changes of this order: active tectonics, migrating warmer or cooler fluids, incomplete diffusion of salt that is excluded from the hydrate structure out into the pore waters, or changes in bottom water temperature and sea level during glacial cycles. The predictions of our equilibrium model must be viewed in the context of this natural variability.

3. Previous Studies of Gas Hydrate Formation in Porous Media

Experiments show that porous media modify the stability of clathrate hydrates according to the pore size and surface properties of the host material [Makogon, 1981; Sloan, 1990; Yousif and Sloan, 1991; Handa and Stupin, 1992; Zakrewski and Handa, 1993; Bondarev et al., 1996; Makogon, 1996; Melnikov and Nesterov, 1996]. The porous medium decreases the stability

range of hydrate. A greater pressure or a lower temperature is necessary to form the hydrate, and a lower dissociation temperature is observed on warming, than is the case under bulk conditions. Values of up to 8°C are reported for the depression in melting temperature of gas hydrates in microporous silica glass [Handa and Stupin, 1992]. Similar values were found for experiments in clay by Melnikov and Nesterov [1996]. Bondarev et al. [1996] found that the melting point of tetrahydrofuran hydrate in loam was decreased by up to 2°C.

Handa and Stupin [1992] concluded that the hydrate in a porous network behaves in much the same way as ice, a premise we develop later. Both Handa and Stupin [1992] and Melnikov and Nesterov [1996] show that the enthalpy of formation of gas hydrate is decreased in porous media, and this is in the same proportion as measured between bulk ice and pore ice. The induction time for hydrate formation in porous media is reduced with respect to formation in free solution, and agitation is not required to induce nucleation of hydrate [Makogon, 1981; Yousif and Sloan, 1991]. This is attributed to the large gas-water surface area in these experiments.

We argue that none of the previous experimental studies can be applied directly to the marine subsurface. One problem is that the porous matrix used was rigid and/or had an unrealistic influence from surface properties due to its composition, or the presence of a fresh rather than saline pore water, which leads to marked expansion of the bound-water layer. The particular physical conditions employed, and the phase distributions that prevailed in these experiments are also different from those likely to apply in situ. Yousif and Sloan [1991] assumed that the presence of a free gas phase within the porous network is needed to form the clathrate, and they ignore the thermodynamic effects of confinement in pores on the hydrate phase itself. Handa and Stupin [1992] considered a water or ice-saturated medium in equilibrium with an external gas pressure. With a 7 nm pore size, capillary pressure on the liquid-water interfaces is so high as to prevent intrusion of free gas into the porous network. Equal

pressures may thus be assumed for the external gas and for the water inside the pores, but there is no direct control of the water pressure.

Submersible experiments overcome some of the problems encountered in replicating in situ conditions in the laboratory. In experiments reported by *Brewer et al.* [1997], methane gas was bubbled through tubes containing coarse and fine sediments. In the coarse sediment, gas flow spread out and hydrate precipitated widely within the pore space, cementing the sediment into a solid mass. In the mud sample, gas flow was restricted to a few channels formed as gas stringers pushed up through the sediment. Gas hydrate precipitation was initially limited to the sides of these "pipes" and a few localized pockets, and then these pore spaces and fractures formed by the passage of gas began to fill with hydrate. These experiments model conditions prevailing close to the seabed where the sediment does not experience a significant confining pressure.

4. Observations of Natural Gas Hydrates and Their Host Sediments

4.1. Shallow Cores and Dredge Sampling

Gas hydrates have been recovered from shallow cores in many sites around the world's oceans and deeper lakes [*Kvenvolden et al.*, 1993]. Gas hydrate has been observed as a cement in sands and sandstones (e.g., Kuparuk Sands of Alaska, [*Collett* 1993]). Findings from numerous localities around the world summarized by *Booth et al.* [1996, 1998] show that gas hydrates more typically occur in the form of segregated bodies: lenses, nodules, pellets, or sheets where the host sediment is fine-grained (clays and silts), and apparently only display an interstitial or cementing habit in coarser-grained lithologies [*Booth et al.*, 1996; *Brooks et al.*, 1994; *Ginsburg et al.*, 1993; *Ginsburg and Soloviev*, 1994, 1998].

4.2. Deep Ocean Drilling

4.2.1. Leg 146: Cascadia Margin. Sites 889/890 offshore Vancouver and 892 offshore Oregon penetrated the zone of gas hydrate stability into an underlying zone bearing free gas [*Westbrook et al.*, 1994; *Carson et al.*, 1996; *MacKay et al.*, 1994]. At both sites the top of the free gas layer was found to lie above the depth predicted from bulk stability calculations using the thermal profiles from the holes (40-50 m higher than the pure water-methane phase boundary and 10-20 m higher (perhaps 0.3°-0.6°C cooler) than the likely seawater-methane curve [*Kastner et al.*, 1995; *Whiticar et al.*, 1995]). Sediments at both localities were predominantly fine grained (clayey silts) with occasional sand layers. The sediments are undeformed in the slope basins and apron (shown in Figure 3a), but the underlying accreted material is highly tectonized and has widely variable texture and physical properties.

Small pellets of gas hydrate disseminated in silty clay and occasional massive pieces were observed in the shallow subsurface of Site 892. Geochemical, physical properties and downhole-logging data indicate that gas hydrates are probably disseminated in small quantities throughout the stability zone [*Westbrook et al.*, 1994; *Hovland et al.*, 1996; *Whiticar et al.*, 1996]. There are also indications that hydrates were concentrated at a number of horizons at both sites. Several layers had a "soupy" or mousse-like appearance, and these were interpreted to be horizons where hydrate had dissociated during core recovery

[*Kastner et al.*, 1996]. The soupy layers have on average a coarser texture than the non-hydrated sediments, but the trend is not definitive (A. Camerlenghi, personal communication, 1994.) The "soupy" layers were interleaved with sediments that were overconsolidated, frequently fractured and anomalously dry, with one silty clay sample dried to the point of losing all cohesion so that its texture resembled ground coffee.

4.2.2. Leg 164: Blake Outer Ridge. ODP Leg 164 was dedicated to the study of gas hydrates [*Paull et al.*, 1997], and included a transect of three sites in the Blake Outer Ridge from a region with no discernible BSR (Site 994) to areas with moderate (Site 995) and strong (Site 997) BSRs. Gas hydrates were sampled in many places, chiefly occurring in the form of small crystals dispersed in the sediment. Indirect evidence of gas hydrates was also obtained from logging and geochemical data from all three sites. Chloride depletion profiles suggest that around 1.5-6% of the pore space is filled with hydrate between about 200 and 450 meters below the seafloor [*Dickens et al.*, 1997], while concentrations exceeding 10% of the pore space occur in several depth intervals. Independent estimates from logging show good agreement [*Paull et al.*, 1997].

The lithology in this region is monotonous, consisting mainly of silty clays and calcareous oozes (Figure 3d). The pore sizes of two typical sediment samples were measured by mercury injection [*Lowell and Shields*, 1991]. Pores diameters range from a few nanometres to a few microns, the mode being 80 - 150 nm; Figure 4. Larger pores are provided by cavities in microfossil shells. Zones of increased hydrate determined by the chloride proxy appear to correlate with sedimentary horizons that have a higher content of siliceous microfossils [*Kraemer et al.*, 1997], while G.D. Ginsburg et al. (Ginsburg, G.D., Soloviev, V.A., Matveeva, T. and Andreeva, I., Sediment grain-size control on gas hydrate presence, ODP Sites 994, 995 and 997, submitted to *Proceedings of the Ocean Drilling Program, Scientific Results*, 1999), analyzing grain sizes of the pore-water squeeze samples, identify a weak but positive correlation between the reported degree of freshening and the proportion of coarser silt fractions.

The thermal profiles derived from downhole temperature measurements indicate that the position of the BSR is colder and shallower than that predicted from bulk equilibria, with 1° to 3°C undercooling, corresponding to 30-100 m of depth offset, in the case of the methane hydrate-seawater system [*Ruppel*, 1997]. There is some evidence that the first appearance of hydrate, at around 190 m, is deeper than predicted from in situ gas content measurements (G. Dickens, personal communication, 1998).

4.2.3. Leg 170: Costa Rica. At Site 1041, which lies at 3300 m water depth offshore Costa Rica, gas hydrates were encountered in almost every core recovered between approximately 120-280 m below seafloor, accompanied by strong pore water freshening [*Kimura et al.*, 1998]. Massive hydrate was found in intervals of fractured claystones and siltstones, and thin sheets of hydrate could be observed within the fractures themselves (Figure 3b). The core faces and fracture surfaces also fizzed for several minutes after recovery. Some of the effervescence came from spots of hydrate visible with the hand lens, but in most cases the source was apparently diffuse within the sediment pores. The hydrate-bearing interval contained several volcanic ash layers. In each ash layer there were indications of the presence of hydrate in the pore space. In two intervals the ash was strongly cemented by gas hydrate (with possibly some water ice) so that it was impossible to break without hard blows from a hammer. Once the hydrate had melted, the ash crumbled to fine dust that was rather dry to the touch.

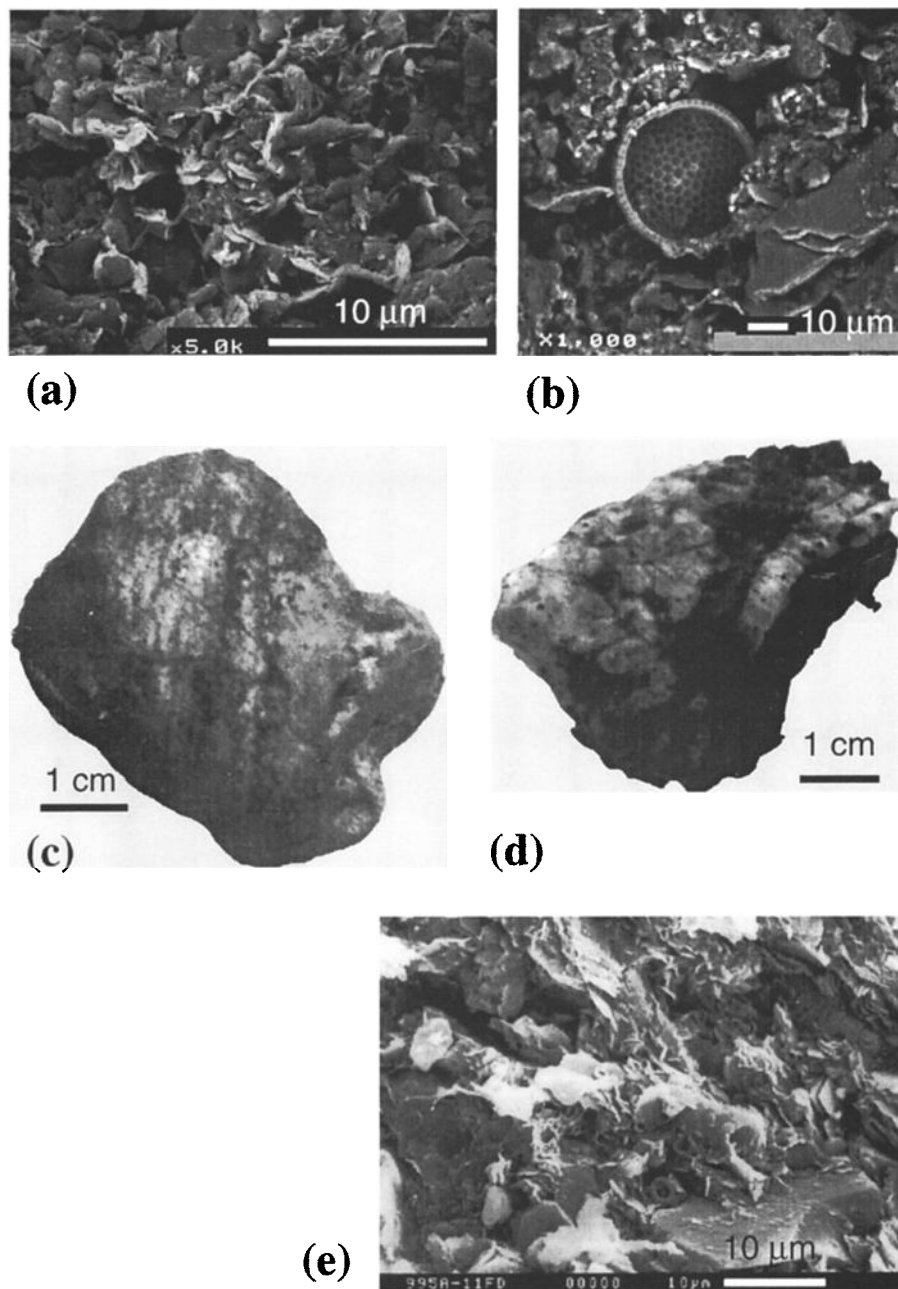


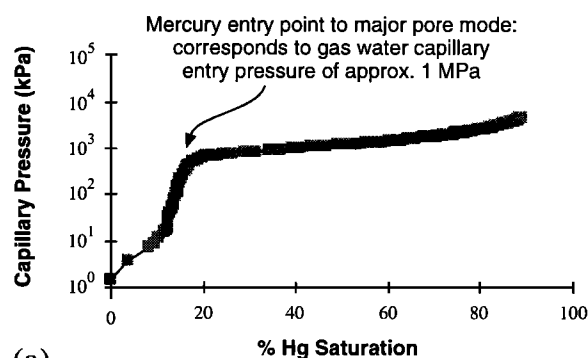
Figure 3. Host sediments of gas hydrates from ocean drilling. (a) Shallow clayey sediment from ODP Hole 892E, 0.5 meters below seafloor (mbsf), Cascadia margin, showing open “honeycomb” pore structure. Conventional scanning electron micrograph. (b) Clayey silt from same hole, 2 mbsf. Low vacuum scanning electron microscope (SEM) image of undried sediment. Note large pores present between aggregates, small pores within particle aggregates, and shelter pores associated with microfossils. (c) Massive hydrate growing either as displacive “lenses” or filling fractures more passively within firm clayey silt, ODP Hole 1041A, 120 mbsf, Costa Rica margin. (d) Banded vitric ash completely cemented by pore-filling clathrate from Hole 1041B, 235 mbsf. (e) Very fine grained silty clay from ODP Hole 995A, 350 mbsf, Blake Ridge. Sediment type is typical of the deeper hydrate-bearing section in this locality. SEM image of freeze-dried sample.

That is, the hydrate cemented the ashy material together (Figure 3c).

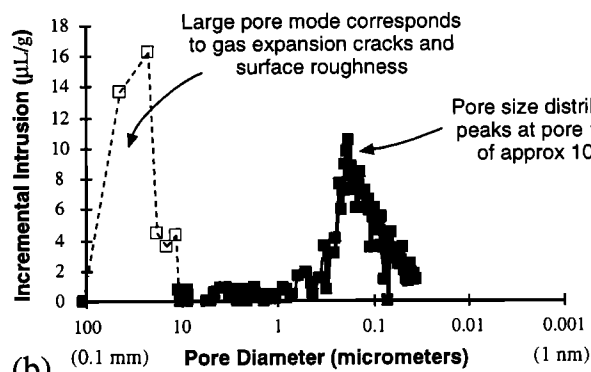
On this part of the Costa Rica margin, the geothermal gradient is so low that the hydrate phase boundary would lie below the maximum depth of drilling. Therefore we have no information from the position of a BSR as to whether the sediment properties were influencing the thermodynamic stability of the hydrates.

5. Thermodynamics in Porous Media

Inside porous media the thermodynamic potential of chemical components can change with respect to bulk conditions as a consequence of (1) Molecular interactions at the pore walls, usually attraction of the fluid molecules by hydrophilic mineral surfaces and (2) The energy required to maintain capillary equilibrium.



(a)



(b)

Figure 4. Mercury injection porosimetry data for clay samples from the Blake Ridge, ODP Hole 995A, 350 and 546 mbsf. Pore-size distribution (volume intruded through progressively smaller pore throats) determined using a cylindrical pore model and the differential of the cumulative volume intrusion curve; mercury surface tension 0.484 N m^{-1} , entry contact angle 140° . Samples were freeze dried to prevent shrinkage.

5.1. Surface Potentials and Depression of Water Activity

Partial ordering and bonding of water molecules with hydrophilic mineral surfaces depresses water activity (activity being a measure of chemical potential normalized to a reference state). *Nitao and Bear* [1996] give a rigorous description of the energy potentials of liquid water in porous sediments. Marked depression of water activity in pores a few nanometers across is attributed to large proportion of molecules being adsorbed on surfaces [Zharikov, 1994].

Depression of water activity is also significant in sediments containing clays, due to their large specific surface area and the pronounced ionic double layer that these minerals develop [Mitchell, 1993] (Figure 5). The consequence is that reactions involving water are inhibited within clay suspensions and in fine-grained sediments. For example, aqueous solutions may become supersaturated within a clay bed, while minerals are precipitated preferentially in adjacent coarser-grained layers in which the pore fluids have normal water activity [Tardy and Novikoff, 1988; Putnis et al., 1995]. We predict that hydrate formation in fine-grained and more clay rich sediments will be inhibited by water adsorption particularly when gas saturation is high. The surface potential effect will add to the osmotic depression in water activity of dissolved salts [Dickens and Quinby-Hunt, 1997] and can be treated in a similar way thermodynamically.

5.2. Capillary Effects

Capillary effects occur when immiscible, mobile phases co-exist within a porous medium. A mobile phase does not have to be a fluid: it can be a deformable solid that flows in order to minimize free energy. Capillary equilibrium is a mechanical balance where a difference in pressure in phases either side of an interface is supported by a surface tension force in the interface region. The interface region has a free energy excess or surface energy associated with it. Surface tension (N m^{-1}) and specific surface energy (J m^{-2}) are dimensionally equivalent, having the same number in SI units. The amount of surface energy in a mass of material is defined by curvature of the bounding surfaces. The total curvature κ of a surface (Figure 6) can be described at any point by the radii r_1 and r_2 of two principal arcs of curvature that intersect orthogonally at that point [Davis, 1996]:

$$\kappa = (1/r_1 + 1/r_2) \quad (1)$$

For each pair of phases (*A* and *B*) in contact within a pore, the difference in phase pressures is the product of the curvature, κ_{AB} , and specific surface energy of the interface γ_{AB} .

$$P_B - P_A = \gamma_{AB} \kappa_{AB} \quad (2a)$$

The pressure difference which exists across the curved phase interface is termed the capillary pressure, and (2) is the Young-

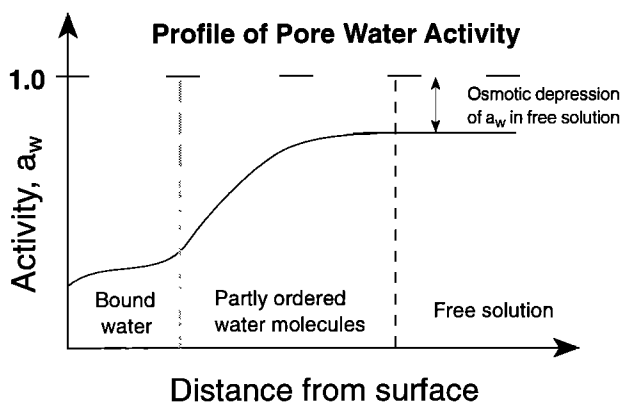
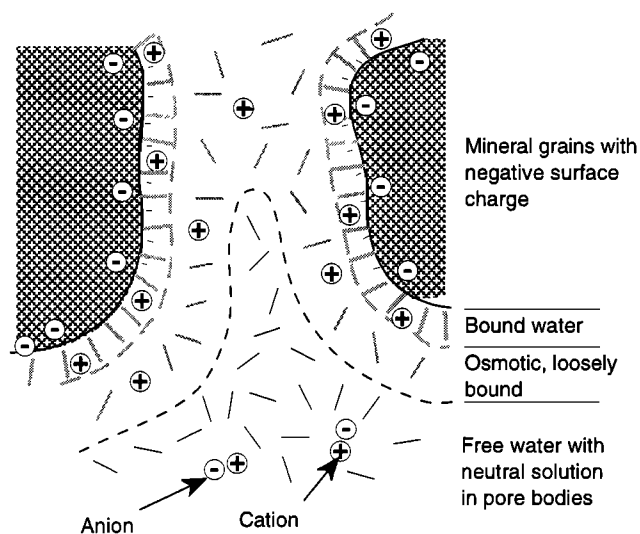


Figure 5. Distribution of capillary, bound and free water in sediment layers and nature of the diffuse bound water layer around clay particles. Based on Mitchell [1993].

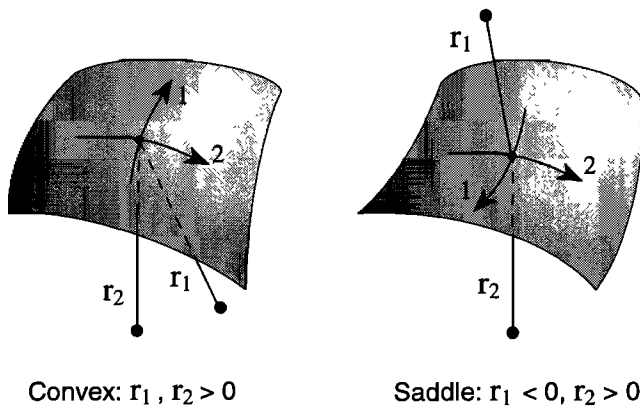


Figure 6. Definition of total curvature and the principal planes of curvature of a surface. The two principal radii of curvature definable at any point may lie on the same side or on opposite sides of the surface.

Laplace equation. On the surface of a sphere $r_1 = r_2 = r$, so the total curvature is $2/r$. On the surface a cylinder of radius r , one of the radii of curvature is infinite, so the total curvature at the walls inside a long, cylindrical pore is $1/r$. However, the end termination of an inclusion within a cylindrical pore is a hemispherical cap, and the curvature of this interface is $2/r$, the same as for an inclusion filling a spherical pore.

The sign convention is such that r_1 and r_2 in (1) are positive when their origins lie in the B phase, so convex inclusions like bubbles have positive surface curvature and positive capillary pressures internally. The relative attraction or repulsion of the fluid phases to the internal surface of the medium, or its wettability must also be specified. Wettability is expressed as a contact angle subtended between the surface and the liquid phase: higher attractive forces give rise to wetting contact angles of less than 90° and or surface films, while non-wetting phases (less attracted than a co-existing wetting phase, or repelled by the molecules of the solid surface) have a contact angle greater than 90° [Davis, 1996]. In a tube or porous medium, the difference in pressure between a wetting A phase and nonwetting B phase (superscripts W and NW , respectively), with the contact angle θ measured through the wetting phase is

$$P_{B,pore}^{NW} - P_A^W = \gamma_{AB} K_{AB} \cos \theta_{surface}^W \quad (2b)$$

The capillary pressure discontinuity across a curved interface represents a mechanical energy balance, but the Gibbs free energies are also affected by surface curvature, by an amount given by the change in surface energy. In differential form, the rate of increase in surface energy is γdA , while the change in surface area A is equal to KdV . The total change in volume is the sum of the changes in partial molar volume of each chemical component in the phase multiplied by the number of moles of that component:

$$dV = \sum_i \bar{V}_i dn_i \quad (3)$$

The change in chemical potential of any one component in a mobile phase can be related to total surface curvature and to the partial molar volume occupied by that component.

$$\mu_i = \mu_i^0 + K\gamma \bar{V}_i \quad (4)$$

Where μ_i^0 is the chemical potential of that component under bulk conditions (zero curvature). A curved inclusion of material, such as a drop of liquid, thus has a higher chemical potential than a large mass of the same substance. The total change in chemical potential of a phase is then given by an extended Gibbs-Duhem equation:

$$dG = -SdT + VdP + \gamma dA + \sum_i \mu_i dn_i \quad (5)$$

Making certain assumptions about the ideality of the fluid phases (perfect gases or dilute solutions) we can make some thermodynamic substitutions and arrive at a general relationship referred to as the Kelvin or Gibbs-Thomson equation that expresses the chemical potential relative to the bulk material as a function of mean surface curvature:

$$\ln \frac{\mu}{\mu^0} = \bar{V}_m RT \kappa \gamma \quad (6)$$

Equation (2) means that small inclusions or convoluted masses with a positive mean curvature, or nonwetting fluids with a convex meniscus in a tube or porous medium have a higher pressure than a surrounding fluid phase. Equation (6) implies that they also have greater chemical activity, higher equilibrium vapor pressure, and greater solubility in solvents than the same substance in bulk. A special form, referred to as the Ostwald-Freundlich equation, is used to express the relative solubility of crystals of different sizes, as explained in section 6.4.

5.3. Freezing Point Depression of Liquids in Porous Media

The freezing point of water is depressed in fine-grained porous media such as soils relative to bulk conditions. This undercooling is an equilibrium thermodynamic effect, observable also during melting, and is unrelated to possible supercooling due to difficulties in nucleation kinetics (see below) that may also occur in bulk water. Undercooling in porous media is attributed to the presence of curved ice-water interfaces that increase the free energy of pore ice relative to bulk ice [Everett, 1961]. Pore water behaves as a wetting phase; most mineral grains are coated with a thin film of water 5-50 nm thick that remains unfrozen, while ice is strongly nonwetting and forms convex shapes within the pores that minimize surface area [Churaev et al., 1993]. The wetting angle between water and mineral grains is effectively zero: that of the nonwetting ice is 180° [Miller, 1980]. Ice has a higher phase pressure than water when they are in thermodynamic equilibrium within a pore.

In the small pores found in a silt or clay sediment, the curvature of the interstitial ice is necessarily great, and the surface energy excess is considerable. Conversely, in coarse sediments like sand the thermodynamic effect is almost negligible because the radius of curvature is large. Figure 7 shows the situation when ice fills a large spherical pore and with further freezing grows into an adjacent cylindrical pore of smaller radius. From the Young-Laplace equation (2b) the pressure of ice in contact with water can be calculated:

$$P_i = P_w + \frac{2\gamma_{iw}}{r_e} \cos \theta_{iw} \quad (7)$$

P_i and P_w are the ice and water phase pressures, γ_{iw} is the interfacial energy per unit area, and r_e is the effective pore entry radius accounting for the unfrozen water film thickness. For this statement of capillary pressure to be applicable, the ice must adopt a curved interface on entry to the pore and there must be a uniform internal phase pressure in the ice [Miller, 1980]. The

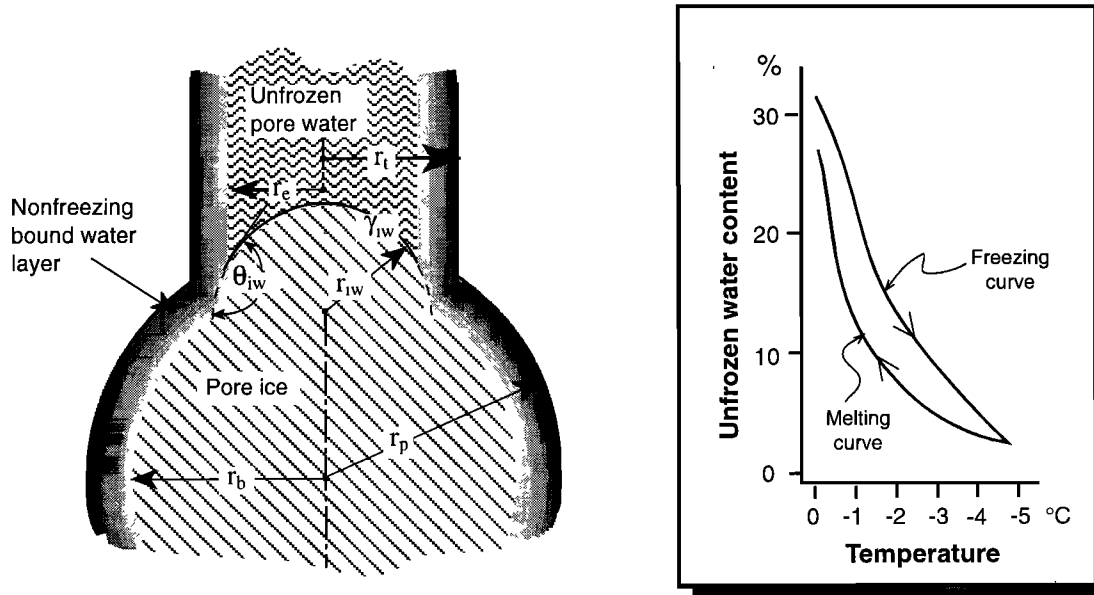


Figure 7. Capillary model of pore freezing. Ice exists within a large pore body (idealized as a spherical cavity), and with further depression in temperature adopts sufficient surface curvature to penetrate an adjacent pore throat (idealized as a cylinder); that is, $r_{iw} = r_e$. Inset, based on *Williams and Smith* [1991], shows the proportion of unfrozen water during freezing and melting; this curve exhibits considerable hysteresis because ice masses in pore bodies (effective radius r_b) are larger than the effective throat sizes (r_e) that must be penetrated for progressive freezing to occur. In our analysis the contact angle for ice θ_{iw} is assumed to be 180° (water wet pores; ice nonwetting).

former assumption is verified by microscopic observations. *Churaev et al.* [1993] and *Adamson and Gast* [1997] refer to experiments where a hemispherical cap rather than crystal faces terminates ice inside small capillary tubes. The convex, rounded, ice-water and ice-air interfaces predicted by *Miller* [1980] are shown in photomicrographs of frozen bead packs [*Colbeck*, 1982]. The second assumption is justified by the low yield strength of ice close to its melting temperature and is known as the “plastic ice” criterion [*Everett*, 1961; *Gunnink and El-Jayyousi*, 1993]. The mechanisms by which pressure is equalized are referred to as solid state creep. *Scherer* [1993] suggests that the main creep process in ice is diffusive mass transfer accompanied by a some intracrystalline deformation.

Combining the Kelvin equation with the Clapeyron equation for the thermodynamic ice-water equilibrium [*Everett*, 1961; *Jallut et al.*, 1992], the depression of freezing point of water in a pore relative to the bulk freezing point can be calculated as a function of the pore entry radius, r_e :

$$\Delta T_{i,\text{pore}} = \frac{2\gamma_{iw}T_{i,\text{bulk}} \cos\theta_{iw}}{\rho_i \Delta H_{f,i} r_e} \quad (8)$$

Here $T_{i,\text{bulk}}$ is the absolute melting temperature of bulk ice (273.15 K), ρ_i the specific density of water and $\Delta H_{f,i}$ the specific enthalpy of fusion of ice. The angle θ_{iw} subtended at the pore wall is 180° if ice is assumed completely nonwetting. A typical clay-bearing silt has pores in the 0.1 μm size range so r_e in eqn. (4) is typically about 10^{-7} m [*Griffiths and Joshi*, 1989]. Substitution of the relevant thermodynamic properties ($\gamma_{iw} = 26.7$ mJ m^{-2} ; $T_{i,\text{bulk}} = 273.15$ K; $\rho_w = 1000$ kg m^{-3} ; $\Delta H_{f,i} = 333$ kJ Kg^{-1}) gives a value of $\Delta T = -0.425^\circ\text{C}$ [*Gunnink and El-Jayyousi*, 1993]. Clayey sediments with bound water layers about 0.5 - 1 nm thick have effective pores sufficiently small (tens of nanometres) to

produce an undercooling of several degrees Celsius (inset graph in Figure 7).

When the temperature increases, it is the effective radius of curvature of the larger pore body, r_b in Figure 7, that determines the melting point of the pore ice. Therefore, depending on the shapes of the pores, considerable hysteresis can occur between melting and freezing curves in porous media [*Jallut et al.*, 1992], and both freezing and melting will occur over a range of temperatures up to the bulk melting point (Figure 7).

5.4. Combining Capillary and Surface Adsorption Effects

The relationship between capillary effects and surface adsorption effects is exemplified by membrane press experiments where an initially saturated soil (or sediment) sample is subjected to a gas pressure [*Bruand and Prost*, 1987; *Tessier et al.*, 1992]. Water may escape from the far side of the membrane and thus is kept at atmospheric pressure. Soils with a rigid framework of sand or silt and those clays with a low specific surface area and layer charge, such as kaolinite, will be invaded by the gas, resulting in capillary equilibrium. On the other hand, fine soils rich in expandable clays such as smectites will compact under the gas pressure, and the small pore size will prevent intrusion of gas up to high pressure (more than 10 MPa). The former type of media are known as solid-solid framework soils, and the latter type are termed colloidal soils [*Miller*, 1980].

These two different responses can both be described as the consequence of changes in water activity, which can be substituted for the chemical potential on the left-hand side of (6). In the solid-solid framework soil the Young-Laplace and Kelvin equations give the equivalence between the maximum size of the water-filled pores, gas capillary pressure, and water activity. In

the colloidal soil, the depression in water activity is the same but is caused by the osmotic effect of the increasingly saline and more tightly bound water remaining in the particle interlayers as fresher water is squeezed out. For example, a maximum water-filled pore radius of 100 μm corresponds to a gas capillary pressure of 1.6 MPa and to a water activity of 0.988 [Tessier *et al.*, 1992]. Water adsorption effects thus appear as an equivalent to capillary effects for compressible materials with very small

pore sizes rather than as an additional effect that should be accounted for separately in the equations [see Henry *et al.*, this issue]. We wish to deal with cases in which hydrate is present in the porous network, and coexists with water, so the capillary description is probably more appropriate. Equally, we must always be aware of the fundamentally different physicochemical and mechanical states that sediments of different mineralogy and texture may exhibit.

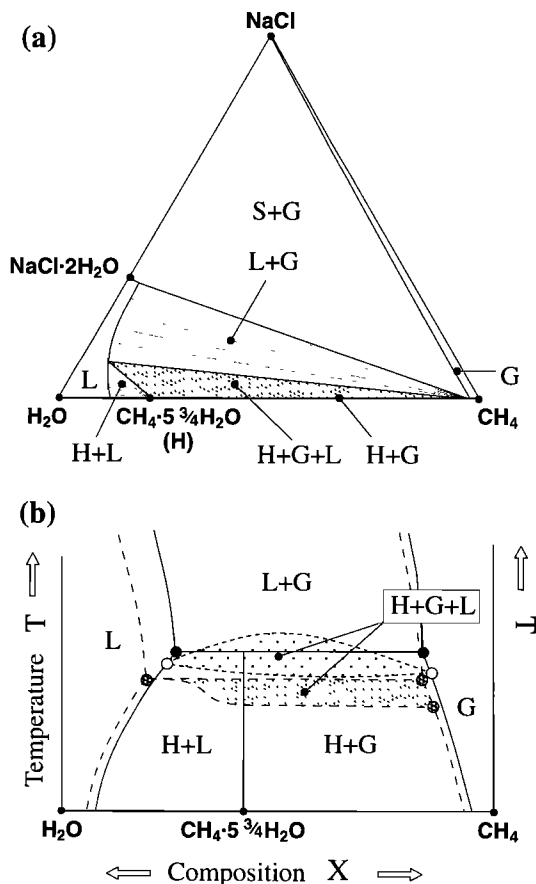


Figure 8. (a) Ternary diagram of the methane-water NaCl system appropriate for the P - T range shown in Figure 1. This is a schematic diagram showing only the topology of phase coexistence and the main univariant and divariant fields. The solubility of methane in water is actually limited to mole fractions of about 0.001 to 0.0025, so the scale in the water rich corner of the diagram is strongly distorted. The hydrate composition shown is approximate for full occupancy of the type I clathrate structure. (b) Schematic T - X section through the ternary diagram for P approximately 20 MPa, and T approximately 10-25 $^{\circ}\text{C}$. Solid lines show the binary system CH_4 - H_2O [see Melnikov and Nesterov, 1993]. The dotted lines show the possible influence of capillarity on the phase equilibrium in the binary system. Water-rich initial compositions require undercooling before pore hydrate can form, whereas in gas rich compositions, capillary supersaturation may promote hydrate stability. Dashed lines apply to a fluid composition containing an appreciable quantity of dissolved NaCl, which decreases the temperature of hydrate formation and leads to “salting out” of a free gas phase [cf., Zatsepina and Buffett, 1998]. At lower temperatures than shown here, salt+hydrate coexistence is possible, and at temperatures below 0 $^{\circ}\text{C}$, water ice and hydrohalite ($\text{NaCl}\cdot 2\text{H}_2\text{O}$) can be stable phases [de Roo *et al.*, 1983].

6. Capillary Model of Gas Hydrate Growth in Porous Media

A simplified phase diagram for the H_2O - CH_4 - NaCl system is shown in Figure 8. According to this diagram, (and a classical interpretation of the Gibbs phase rule), gas cannot exist as a free phase within the zone of gas hydrate stability while water is present in excess except when the pore water is highly saline [Zatsepina and Buffett, 1998]. Were gas to exsolve locally due to ingress or in situ production, it would rapidly combine with water to form more hydrate [Sloan, 1990; Paull *et al.*, 1994]. We examine the two-phase equilibrium between hydrate and methane-saturated water before considering the effects that confinement in sediment has on the [gas + water] / hydrate phase boundary.

6.1. Two-Phase [Hydrate+Gas Saturated Water] Equilibrium

Theory and experiments suggest that hydrate can nucleate and grow from aqueous solutions that are near to saturation or metastably supersaturated with respect to methane, without free gas being present [Handa, 1990; Mashirov *et al.* 1991; Melnikov and Nesterov, 1993; Tohidi *et al.*, 1995; Zatsepina and Buffett, 1998]. The likely kinetic mechanism for the formation of gas hydrate also requires that the methane molecules dissolve in water before they can be incorporated within the clathrate lattice [Lekvam and Ruoff, 1993]. Moving away from the three-phase boundary into the two-phase hydrate-stable region by increasing pressure and/or decreasing temperature reduces the aqueous solubility of methane, resulting in a greater proportion of clathrate for a given amount of total methane present and an increase in occupancy of gas molecules in the clathrate cages [Handa, 1990].

Calculations of the two-phase equilibrium under P , T conditions appropriate for submarine hydrates show that methane solubility decreases upwards from the base of hydrate stability towards the seafloor [Tohidi *et al.*, 1997; Zatsepina and Buffett, 1998]. If methane-bearing waters advect upwards, progressively more gas can be extracted from the water to form hydrate [Rempel and Buffett, 1997, 1998; Ginsburg and Soloviev, 1997]. Even in the absence of fluid advection, the progressive upwards decrease in solubility will also produce a chemical potential gradient tending to draw methane upwards through the hydrate stability zone by diffusion in the pore water [Rempel and Buffett, 1997, 1998].

6.2. Pressures and Temperatures Within the Hydrate Stability Zone

Assuming that water forms a continuous wetting phase in the pores and that the system remains open with respect to transport of methane, salts, and water, then the aqueous phase pressure will be maintained (or buffered) at a value very close to hydrostatic pressure. This assumption is reasonable even in the presence of a modest water flux in a sequence of compacting sediments [X_u

and Ruppel, 1999]. The pore water pressure is then given by

$$P_w = \rho_w g(z + h) \quad (9)$$

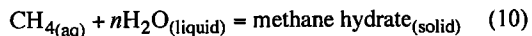
where ρ_w is the density of the pore water, g is the acceleration due to gravity, z is the depth in the sediment column and h is the water depth. In hydrate-stable regions beneath the ocean the hydrostatic pressure of the water will generally range from 5 to 50 MPa.

With water pressure stipulated as the reference pressure in the open-system stability zone, hydrate phase pressure becomes the dependent variable in (2b). The phase pressure of non-wetting hydrate entirely confined within the pore space is given by the sum of the hydrostatic reference pressure and a "capillary" component, dictated by the mean surface curvature of the crystals. The curvature changes in a complex way according to pore size distribution, percentage filling of the pore space, and growth habit, but remains positive. In a finely porous medium the capillary pressure of hydrate may be a significant proportion of the total pressure. For example, if the surface energy for hydrate is similar to that of water ice, about 30 mJ m⁻², we find that in a cylindrical pore of 50 nm radius, the capillary pressure of hydrate will be of the order of 1 MPa.

We have assumed, loosely, a linear thermal gradient through the sediment pile. This implies that heat flow and thermal conductivity are constant with depth, there is negligible advection of heat by moving pore fluid and that the reaction to form hydrate itself does not perturb the thermal structure (i.e., there is a kind of static equilibrium). The water chemical potential is then a predictable function of depth while open-system equilibrium prevails. The sediment pore size and mineralogy may vary from place to place within the sediment, leading to different contributions to the energy state of the water from surface interactions. However, these perturbations can be balanced by minor variations in salinity and microscale fluctuations in fluid density that equalize the overall chemical potential [Miller, 1980; Nitao and Bear, 1996]. This is why we consider the water phase to be "buffered" in a reference state in an open system.

6.3. Capillary Inhibition of Gas Hydrate Growth in Porous Media

According to the preceding analysis for ice, hydrate formed inside pores is less stable than bulk hydrate. The formation of clathrates in the two-phase region is inhibited by capillary effects, and an extra thermodynamic drive is required to promote the reaction whereby water containing dissolved methane converts to solid gas hydrate:



Here n is a stoichiometric coefficient, equal to about 5.75 for full occupancy of Type 1 methane hydrate, Sloan [1990]. We suggest three possible ways to overcome the inhibition:

1. Undercooling with respect to the bulk equilibrium temperature at a given pressure, because reaction (10) is exothermic.
2. An extra pressure on the liquid phase reactants relative to bulk equilibrium at a given temperature because reaction (10) involves a net volume loss ($\Delta V < 0$) under likely P, T conditions.
3. Supersaturation of the aqueous solution with respect to methane.

Condition 1 can be achieved if the base of hydrate stability migrates upwards in the sediment column. This would produce a shallower than normal BSR where gas is present in excess of

solubility in that part of the sediment column. Condition 2 could be achieved if the pore fluids are overpressured; though this violates the assumption of hydrostatic pressures and open system conditions. Condition 3, supersaturation of methane in the pore water, could occur if formation of gas bubbles is also inhibited by capillary effects. The behavior of a free gas phase is considered in section 6.7. Within the two-phase region, the requirement for supersaturation means that less hydrate will form for a given amount of gas, and the threshold amount required to form hydrate at any depth [Handa, 1990] will be reduced. The first appearance of hydrate going down into the sediment is controlled by the balance of methane production and upwards flux to a sink in the zone of methane oxidation close to the seabed [Borowski et al., 1996]. The depth where methane first reaches the threshold amount to precipitate hydrate will be deeper in a sediment pile affected by inhibition than would be predicted by a bulk thermodynamic model [Tohidi et al., 1997].

6.4. Nucleation of Hydrate Inside Porous Media

To form hydrates, dissolved gas molecules must combine together with water molecules in a cluster of sufficient size for the free energy change of the reaction to overcome the surface energy of the new interface. The cluster of critical size has an energy excess that just balances the excess chemical potential of the reacting components. This cluster is the nucleus for further growth, which is energetically favorable because the excess chemical potential of the crystal decreases as its radius increases. In hydrates, the thermodynamic drive to overcome the energy barrier associated with nucleation comes from supersaturation of the water with methane. Supersaturation may result from increased supply of methane, increased pressure, or reduced temperature. We can express this relationship between cluster size and supersaturation using the appropriate form of the Kelvin equation:

$$\ln \frac{S^r}{S^0} = \frac{2\gamma \bar{V}_m}{r RT} \quad (11)$$

S^r is the saturation of the pore fluid in equilibrium with nucleating crystal of radius r , while S^0 is the bulk solubility, or saturation at equilibrium with a flat surface.

The two possible mechanisms for appearance of a new phase are homogeneous nucleation, where a cluster forms in the body of the liquid, and heterogeneous nucleation, where the cluster forms on a third surface such as a gas bubble or a mineral substrate [Adamson and Gast, 1997]. The level of supersaturation required for homogenous nucleation is normally much greater than that required for heterogeneous nucleation.

Drawing analogy with the freezing of water [Scherer, 1993] and the crystallization of salts [Putnis et al., 1995] inside porous media, we believe that it is extraordinarily unlikely for homogeneous nucleation of hydrate to occur in isolated small pores. We consider that homogeneous nucleation and efficient growth under diffusion-limited conditions can only occur in larger pores or fractures, and then the maximum degree of inhibition is not set by the pore size of sediments but by the size of the critical hydrate nuclei.

For ice, the radius of the critical nucleus is about 2 nm, but this will not appear until a supercooling of up to 40°C is attained [Churaev et al., 1993]. In gas hydrate reactors, the size of first-formed nuclei is estimated from laser light scattering to be 5-30 nm [Higskole et al., 1994]. Chersky and Mikhailov [1989] calculate the equilibrium size of the first-formed nucleus for

clathrates. For a supercooling of up to 10°C they predict a critical radius for hydrate in equilibrium with methane-saturated water of about 7 nm, and for a supercooling of 1°C a radius of approximately 70 nm. Thus in the absence of a significant thermodynamic drive from supersaturation there may be a space problem when nucleating methane hydrates within the pores of compacted clays and silts that are only tens of nanometres across [Ginsburg and Soloviev, 1998].

A further restriction on nucleation of hydrates in porous media (pointed out by an anonymous reviewer) arises when the gas supply to maintain supersaturation is not strong. This limits the amount of methane available in the ambit of small pores to form a critical nucleus. Given the r^3 relationship between pore radius and volume and the sensitive dependence of nucleation probability on the numbers of freely associating molecules [Adamson and Gast, 1997], it seems that pore size could exert a very strong constraint on nucleation even when the pores are much larger than the critical size for homogeneous nucleation.

Experimental observations of short induction times [Yousif and Sloan, 1991; Makogon, 1981; Melnikov and Nesterov, 1996], together with the arguments just outlined, suggest to us that heterogeneous nucleation in larger pore spaces is the norm when gas hydrate grows in porous sediments and rocks.

6.5. Progressive Growth of Gas Hydrate in Porous Sediments

After nucleation the hydrate crystal will go through a period of rapid growth. If local equilibrium prevails and methane is continually replenished, then hydrate will continue to form, almost uninhibited, and fill any larger pores or fractures already present in the sediment. After this period, the crystals will impinge on the pore walls and necessarily adopt greater surface curvature as interstices are filled and smaller throats penetrated. According to (11), this restricted growth stage requires progressively greater supersaturation, from cooling or an increased methane supply.

Consider the following scenario with reference to the phase diagram shown in Figure 8. For small amounts of gas dissolved in the water (to the left of the field marked L) no hydrate can form. As the amount of methane originally present in the pore water increases, hydrate forms first in the largest pores, in equilibrium with a fluid strongly depleted in methane. After equilibrium is established at a particular depth, more methane entering the system will at first convert directly to hydrate, but then build up in the pore water until the supersaturation is sufficient to drive the hydrate into smaller and smaller pores.

6.6. The Segregation Criterion and Role of in Situ Stresses

When the space in all voids larger than a certain size is filled, the hydrate will tend to grow as a displacive inclusion or a segregated layer rather than penetrating into smaller and smaller pores (Figure 9). The mechanical condition for segregated growth is met when the phase pressure exerted by the hydrate P_h exceeds the effective confining stress (σ_0) plus the tensile strength of the sediment (E_s). It is given by [cf. Scherer, 1993]:

$$P_{h,seg} = P_w + \gamma_{hw}(\kappa_e - \kappa_p) \geq \sigma_0 + E_s \quad (12)$$

where κ_p is the surface curvature of the existing hydrate in the pore bodies and κ_e is the curvature required for the next smallest throat to be penetrated. The effective confining stress is somewhat less than the vertical lithostatic stress at a particular depth, as it depends on the stiffness of the sediments and

anisotropy of the in situ stresses. The cohesion of uncemented sediment is generally negligible with respect to the confining stress, but lithified sediments may have a tensile strength of several megapascals. The segregation criterion in (12) will only be met where there is a wide range in pore sizes including pores with very narrow throats; that is, in clays and silts, where pore sizes will be in the nanometers to micron range. In sands and other media with coarse texture, the segregation criterion is not met even as hydrate enters pore throats, and so according to our model clathrate will continue to grow as an interstitial phase.

At some depth the mechanical energy required for segregated hydrate growth may become greater than the energy saving conferred on the segregated hydrate by virtue of its small surface curvature. We speculate that if early-formed hydrate can flow under stress like ice, it could be squeezed into smaller pores as it is buried in the sediment pile. Over time, it is possible that an annealing process could occur whereby small hydrate crystals are dissolved preferentially to be redeposited as segregated masses [Everett, 1961]. Yardley [1975] discusses such a mechanism for the formation of segregated mineral veins that grow at the expense of a finer groundmass. The equation describing the chemical potential of the mineral grain ($\mu_{m,grain}$) is

$$\mu_{m,grain} = \mu_{m,bulk} + \bar{V}_m \gamma_{m,\alpha} \left(\frac{dA}{dV} \right) + (w_e + w_p) \quad (13)$$

The first term on right-hand side is the bulk chemical potential of the substance (unstrained, no surface curvature). The second term is a positive free energy contribution arising from surface area, where \bar{V}_m is the molar volume, $\gamma_{m,\alpha}$ the interfacial energy per unit area (or surface tension) of the mineral with respect to the surrounding fluid phase, here denoted α . The terms w_p and w_e are plastic and elastic strain energy terms for internal crystal strain and reaction against the confining stresses of the surrounding sediment. If hydrate is like ice we can probably neglect internal strain energy [Everett, 1961], so that (13) is a thermodynamic balance reflecting the mechanical equilibrium expressed by (12). Together these can be used to relate the mechanical forces mobilized by a growing curved crystal to the thermodynamic drive available from undercooling and supersaturation.

6.7. Role of Free Gas

If sufficient methane is present in the system to exceed solubility in the pore water (compositions starting in the L+G region of Figure 8) then free gas will be present at and below the phase boundary. It is also possible for gas to be present as a stable or metastable phase within the zone of gas hydrate stability under certain circumstances. As explained by Zatsepina and Buffett [1998], free gas can exist even on the water rich side of the hydrate bulk composition if the porewater is sufficiently saline; this hydrate + liquid + gas stability field is shown as the shaded triangle in Figure 8a. Water depletion (and accompanying salt buildup) in a partially closed system can move the fluid composition from the normal hydrate + liquid field into the H+L+G field. The base of the hydrate zone will then contain a depth interval where all three phases can coexist. In a traverse through the three phase region, the hydrate proportion increases progressively upwards.

The interfacial energy of water with methane is around 70-72 mJ m⁻² [Tissot and Welte, 1978]. If hydrate has properties similar to ice its interfacial energy with water will be around 30 mJ m⁻². The internal pressure inside a hydrate crystallite of radius 0.1 μ m will then be approximately $2 \times 3 \times 10^{-2} / 1 \times 10^{-7} \text{ m} = 600 \text{ kPa}$

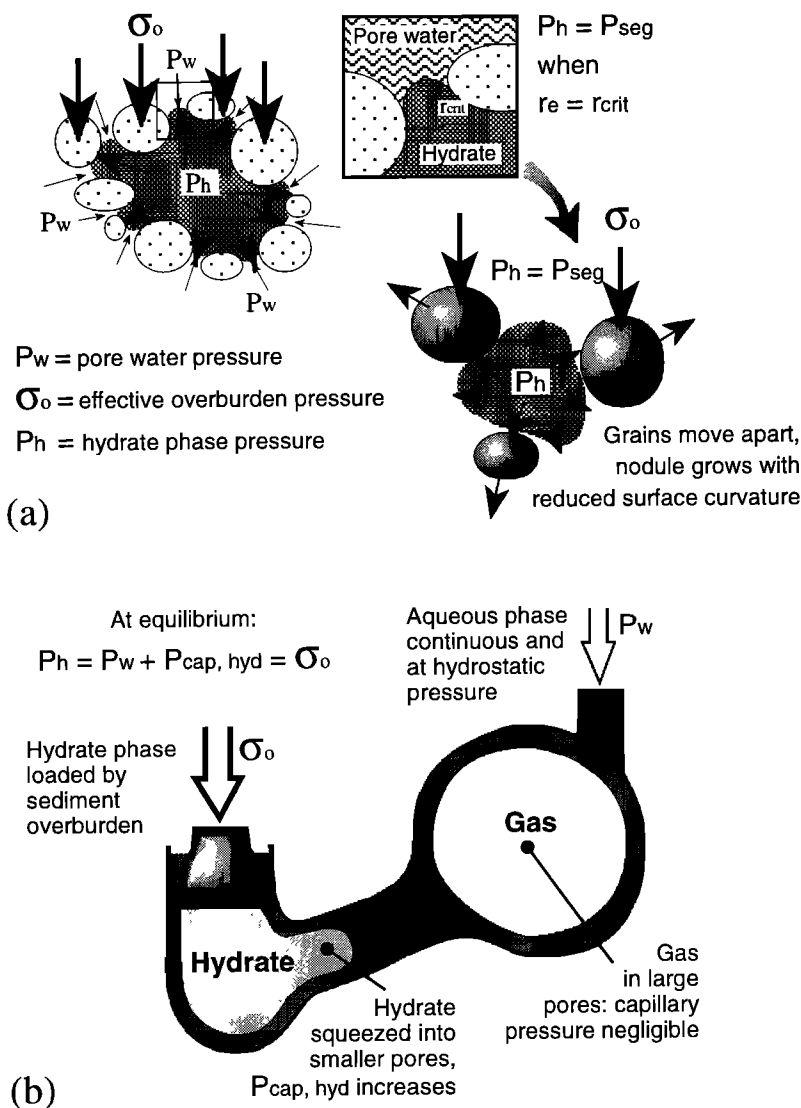


Figure 9. Explanation of gas hydrate segregation. (a) Hydrate grows as an interstitial phase when it can adopt a stable surface curvature that allows it to penetrate pore throats. When this curvature is greater than a certain value (i.e., all pore throats greater than a critical size have been penetrated), then the hydrate pushes aside the sediment grains and grows displacively. This happens when the surface curvature enforces a phase pressure inside the solid that exceeds the yield strength that can be mobilized by the sediment matrix. (b) Relationship between lithostatic load, pore size and hydrate phase pressure. The lithostatic pressure of overlying sediments is shown schematically as a weight pushing down on the segregated hydrate. At equilibrium the crystal generates a higher internal pressure to balance this force, enabling it to adopt greater curvature and extrude into smaller pores. Circumstance illustrated where gas bubbles, having higher surface energy, occupy larger pores than hydrate crystals; the segregation process itself is not dependent on free gas being present.

greater than the surrounding pore water, while a gas bubble of the same size would have a capillary pressure of 1400 kPa. Gas will therefore tend to occupy larger pores in the three-phase zone, and the phases will reconfigure to minimize the total surface energy (Figure 10).

In the marine subsurface we have assumed that the liquid phase is continuous and wetting to the sediment grains and that its pressure is hydrostatic. The gas pressure exceeds the coexisting water pressure by an amount that depends upon the size of free gas bubbles and/or the curvature enforced by their confinement inside pores. At thermodynamic equilibrium, the requirement for the chemical potential of dissolved methane to equal that within

small bubbles of the gas phase leads to an increase in the concentration of methane in water. This effect, which has been discussed by Kamath and Boyer [1995], Claypool [1996] and Makogon [1996], is termed capillary supersaturation. The thermodynamic potentials of the various chemical components change according to the internal pressures of the phases that they are in (interfacial curvature of the bubble and gas fugacity inside it are related by the Kelvin equation), so changes in the gas capillary pressure will influence the hydrate-forming reactions. Methane supersaturation promotes hydrate formation, that is, it counteracts the capillary inhibition of hydrate in pores [see Henry *et al.* this issue].

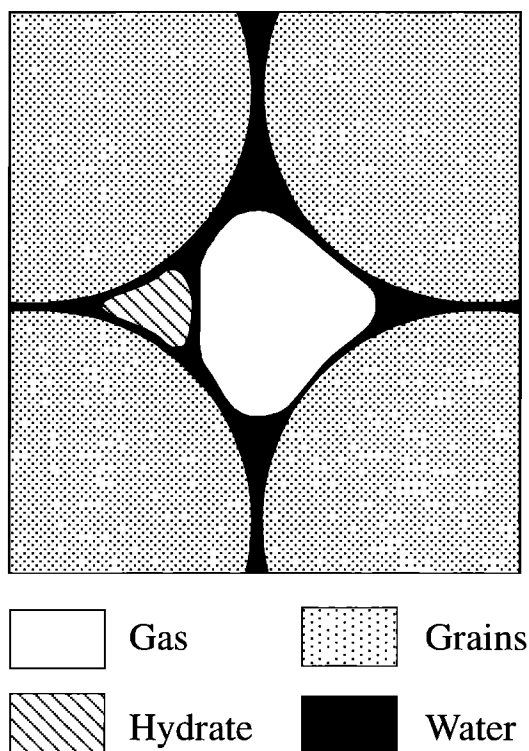


Figure 10. (a) Distribution of coexisting gas, hydrate and water in pores at thermodynamic and capillary equilibrium for a framework-supported sediment. We assume the water has an affinity for the solid surfaces and is completely wetting, and that the gas phase is completely non-wetting to pore surfaces. The hydrate is assumed to behave like ice and to be completely non-wetting, but with $\gamma_{hw} < \gamma_{gw}$. In order that capillary forces balance in a circuit around phase interfaces we find the relation: $\gamma_{hg} = \gamma_{gw} + \gamma_{hw}$. Under these circumstances the distribution of phases when they are able to coexist (i.e., at thermodynamic equilibrium) will be arranged so that water forms a continuous film on the pore walls, and the highest energy interfaces between gas and solid clathrate are completely avoided. The configuration shown represents a critical hydrate proportion in this pore (a stability limit) Further growth of the crystal would mean an increase in the gas bubble curvature that would lead to further gas dissolution, and disappearance of the bubble from the pore, while the larger hydrate crystal becomes more stable due to lower surface curvature, and can accept more gas from solution. That is, the subsystem jumps from a state where three phases are stable, to one where only hydrate + liquid can coexist. Based on *Miller*, [1980].

6.8. Importance of the Total Amount of Methane in the System

Large changes in the proportion of methane present in the starting composition will move the system between different fields in the bulk stability diagram (Figure 8a), producing different histories of phase coexistence as the fluid is cooled or warmed. Only in relatively methane-rich fluids will free gas ever appear, while for starting compositions rich in both gas and salt, cooling will involve a traverse through a region of three-phase coexistence before the hydrate + liquid divariant field is reached. Confinement in a porous medium adds complications. In a sediment with a distribution of pore sizes, the pressure inside growing inclusions of either gas or hydrate will rise as the

percentage of pore space that they occupy increases. Thus the internal pressures of gas and hydrate are a function of temperature, pore-size distribution, and the starting composition, not just depth below sea level. Reactions depend on phase pressures, so rearrangements may be necessary for the system to maintain both thermodynamic and mechanical equilibrium as hydrate grows or melts.

It is possible that even in the binary system CH₄-H₂O the phase boundary ceases to be a univariant line and becomes a divariant region where gas + liquid + hydrate may be stable. An extra degree of freedom, namely, phase saturation, is introduced into the system. The behavior parallels that of the ternary system with salt present, but in the capillary case the increased variance comes not from an increase in the number of components but from the fact that the gas pressure no longer has to equal the water “reference” pressure. Figure 8b is an attempt to sketch the T-X section of the binary system.

Where there is a three-phase stability zone, the first appearance of free gas bubbles when going downwards into the sediment need not in general coincide with the last appearance of hydrate, even when the salinity is not unusually high. The first appearance of gas, and so the position of the bottom simulating reflector, will depend upon the level of capillary supersaturation. This in turn will be a function of the pore-size distribution in the host sediment and the total amount of gas in the system. Thus, according to our model, the BSR could be encountered at various depths in the same sediment type according to the amount of methane present at that locality.

Capillary pressure-saturation curves for sediments invariably exhibit hysteresis: pore bodies are linked by narrow throats [*Griffiths and Joshi*, 1989; *Jallut et al.*, 1992]. This implies that different conditions of phase saturation, pressure, and temperature will prevail in the three-phase zone depending on whether, over time, the base of hydrate stability is moving up or down relative to the sedimentary strata, and this will affect the BSR position [see *Pecher et al.*, 1998].

We now consider the possibility of overpressure in the reference pore fluid caused by compaction disequilibrium, high basal fluid flux, or some other mechanism. An increase in water pressure above hydrostatic will lead to an similar increase in the gas phase pressure in order to maintain capillary equilibrium. The chemical potential of the methane component thus increases with the rise in the pore water pressure, so promoting the forward reaction to produce hydrate, even if there is no increase in the total amount of methane [*Handa*, 1990]. The volume of hydrate need not necessarily rise proportionately as this happens, some of the methane squeezed out of solution may go to increase the percentage occupancy of gas in the hydrate lattice.

6.9. Hydrate Growth in a Partially Closed System and Sediment Water Depletion

Growth of hydrate in concentrated layers or in nodules will sequester water and gas from surrounding sediments in a way analogous to ice lenses in frozen soils [*Miller*, 1980; *Clelland et al.*, 1995]. The effect on the surrounding sediments depends on the speed of hydrate growth relative to the rates at which water and gas are supplied by transport through the sediment and the excluded salts are diffused away [see *Ussler and Paull*, 1995]. Hydrate growth rate will also depend on heat transfer, but considering that the diffusion of heat (typically, 10 m² yr⁻¹) is about 500 times faster than diffusion of either salt or methane (typically, 0.01-0.02 m² yr⁻¹) [*Iversen and Jorgensen*, 1993], salt buildup is likely to be the limiting factor.

We speculate that where the permeability is low and gas supply (in situ microbial production plus influx) is high, there will be a thermodynamic drive to draw pore water from surrounding sediments at a rate greater than it can be replenished. This "suction" on the pore fluid will increase effective stress and lead to consolidation the sediment. *Konrad and Duquenois* [1993] explain such a process when ice segregates during soil water freezing, though we appreciate that the analogy is not perfect because in the case of clathrate growth the water is probably sequestered because of local gas excess rather than through thermodynamic undercooling (G. Ginsburg personal communication, 1998; A. Rempel personal communication, 1998). Cores recovered from a water-depleted sequence may show marked excursions in physical properties between dry and stiff water-depleted horizons and anomalously wet layers (soupy or moussy texture) where preexisting gas hydrate had melted.

Ginsburg and Soloviev [1997] stress that advection of pore water containing dissolved gas and transport of methane as a free gas phase are fundamentally different scenarios. In the former case water is supplied along with the gas, and hydrate precipitation is somewhat akin to freezing of a water stream. In the latter case, gas is in excess of its proportion in hydrate and water must be drawn from the surroundings for the reaction to proceed. In mud volcanoes or other areas of focused gas flow, the sediment around the gas pathways may become dried out and lined with hydrates. This "frozen" barrier allows the passage of more gas through the conduit without it combining with water to form clathrates [*Ginsburg and Soloviev*, 1997].

We speculate that in extreme cases of "freeze drying," the residual water may be present only as capillary water in interstices or as films adsorbed on sediment particles. The low chemical potential of this residual water (Figure 5) may prevent its reaction with gas to form more hydrate under the prevailing conditions. Through this water depletion mechanism, small quantities of free gas may be trapped in dry, hydrate-bearing sediments, perhaps leading to seismic blanking or locally affecting the seismic expression of the BSR. If salt builds up during this "gas flushing," a fringe of brine may surround patches of hydrate, and this would draw in water osmotically from surrounding sediments [*Mitchell*, 1993; *Konrad and Duquenois*, 1993]. The more active a methane venting system is, the further it can be pushed from equilibrium. For example, the water and solute contents of the sediments sampled from active mud volcanoes may be very heterogeneous [*de Lange and Brumsack*, 1998].

The amount of gas necessary for water depletion is considerable. To dry a sediment of 50% original porosity down to the point where all the water is bound to particle surfaces (say 10% water content) requires removal of 400 kg of water, and so a supply of nearly 75 kg methane, for each cubic meter of sediment. For a sediment organic carbon content of 1% that is converted to methane by bacteria with 10% efficiency [e.g., *Waseda*, 1998], the amount of methane required for drying is about 50 times greater than could be supplied in a closed system.

6.10. Predictions of the Capillary Model

Our conceptual model predicts six main phenomena that can be tested by observations of natural gas hydrate systems:

1. Upwards displacement of the BSR in fine-grained sediments due to inhibition of hydrate nucleation and growth. In the companion paper, *Henry et al.*, [this issue] quantify this effect.
2. Capillary inhibition will increase the depth below the

seafloor at which hydrate is first encountered and reduce the amount of methane partitioned into hydrate at any depth.

3. (a) Formation of segregated hydrate in fine-grained sediments, and interstitial hydrate in coarser sediment layers. (b) Suppression of this tendency at greater depth where overburden pressure may squeeze hydrate into small pores.

4. With a partly closed-system or high gas flux: (a) Water depletion in the vicinity of concentrated hydrates. (b) Haloes of saline water around growing hydrate due to incomplete diffusion of excluded salt.

5. Free gas pockets within what would normally be the hydrate two-phase region. These may be detectable from low sonic velocities and seismic blanking.

6. (a) Hysteresis in the physical conditions of gas hydrate first and last appearance during formation and melting in the sediment. (b) Different phase proportions at a given temperature and pressure in the three-phase region according to whether the sediment mass is moving, relatively, into or out of the thermodynamic region of clathrate stability.

7. Discussion of the Capillary Model

7.1. Unknown Surface Properties of Clathrates

There are no reliable published values for the interfacial energy of hydrate; nucleation phenomena are very sensitive to the exact value of surface energy [*Davis*, 1996]. Recent molecular dynamics simulations reveal that our notions of interfacial energy and wettability are a simplification of a rather complex system [*Rodger et al.*, 1996; P. M. Rodger, personal communication, 1996 and 1997]. Nevertheless, experiments on the critical size of hydrate nuclei in aqueous solution [*Higskole et al.*, 1994] and structural considerations both suggest that the effective hydrate/water interfacial energy is similar to that of ice (Y. P. Handa, personal communication, 1995 and 1997; K. Lekvam, personal communication 1996), and we use this value here and in the companion paper [*Henry et al.*, this issue].

7.2. Effects of Host Sediment Surface Chemistry

Cha et al. [1988] and subsequently *Ouar et al.* [1993] reported that clay suspensions can promote the rate of hydrate growth and its equilibrium thermodynamic stability relative to bulk conditions. However, experiments conducted by *Englezos and Hall* [1994] found no enhanced effect from montmorillonite surfaces and confirmed the finding that most organic and inorganic materials acted to inhibit hydrate formation. While it is possible that certain mineral surfaces can promote heterogeneous nucleation of hydrate, it is less certain that they can increase its thermodynamic stability significantly. *Carlisle* [1983] suggested that hydrate nucleation would be favored by partial preordering of water molecules into tetrahedral coordination adjacent to strongly hydrophobic surfaces. Most minerals found in marine sediments are hydrophilic, but there is some evidence that organic substrates such as kerogens or biofilms may possibly promote hydrate precipitation.

Van Kesteren and others report that anomalously large amounts of propane will dissolve in clay slurries compared with the solubility in water at the same P and T ; hydrate formation appears to be promoted also. This is interpreted either as adsorption of gas molecules on the mineral surface and/or capillary supersaturation (W. G. M. van Kesteren, personal communication, 1998). It is not clear how similar the behavior of methane would be to the larger propane molecule.

7.3. Controls on Gas Hydrate Growth Forms

The development of faceted rather than curved crystal faces (implicit in our model) is likely for crystallites above a few microns in size [Adamson and Gast, 1997], but the qualitative behavior we describe will be the same so long as the clathrate growth forms remain convex and compact [see Everett, 1961]. Compact growth habits are often favored when a mineral grows slowly from solution at a low degree of supersaturation [Cody, 1991; B. Yardley, personal communication, 1996]. Such forms were observed recently in Structure I methane clathrate crystallites by Smelik and King [1997].

Taking the available observations at face value, it would appear that massive or "segregated" hydrate growth forms predominate in fine-grained sediments, but that sometimes fine sediments can host clathrates that are widely distributed and "diffuse" in the sediment (e.g., Blake Ridge and Costa Rica Margin). We note that fine-grained sediments predominate in deep marine environments and that most hydrate samples that survive through core recovery to the time of inspection will necessarily be biased toward the larger masses. On the other hand, apparently diffuse hydrate in fine sediments may in fact consist of small nodules or inclusions (10 μm to 1 mm across). Although invisible to the naked eye, these hydrate particles are considerably larger than the pores and so, in terms of our model, have a segregated habit.

The capillary model predicts that deeper in the sediment column, hydrate could be squeezed into smaller pores, with nodules exhibiting the effects of pressure solution. This type of behavior is evident in sediment-hosted anhydrite nodules [Machel and Burton, 1991]. The loose analogy between sulfate minerals and gas hydrate nodules is prompted by their remarkably similar appearance, at least at the scale of hand specimens (compare photographs in Peyrt *et al.* [1993], with [Sloan, 1990, p. 411] and Kvenvolden *et al.*, [1993]).

Kastner [1970] and Shearman [1981] studied the factors that control whether gypsum crystals grow to envelop sediment particles, so forming a poikilotopic cement, or alternatively push sediment particles aside during growth. Rapid growth was found to favor overgrowth, whereas slow growth favors particle displacement and segregation: clearly the force of crystallization that can be mobilized depends partly on kinetics, not just on pore size. Studies on the growth of ice in a matrix of silica particles reported by Scherer [1993] also demonstrate that crystals will engulf rather than push aside particles when growth is rapid. This occurs at negligible effective confining stresses and despite the fact that ice is strongly nonwetting to silicates. The critical growth speed is determined by the rate at which water can be transported into the gap between the face of the crystal and the displaced particle. We speculate that interstitial forms of hydrate may attest to relatively rapid growth, and so a high degree of undercooling and/or supersaturation of the pore fluids with methane. In contrast, nodular forms of hydrate may suggest that the nucleation of hydrate and its rate of growth have been reduced by inhibitors [Cody, 1991], restricted transport of reactants [Putnis *et al.*, 1995], or slow production rates of methane.

Several authors suggest that annealing during melting and recrystallization cycles may be important in concentrating hydrates into particular layers [Malone, 1985; Yousif and Sloan, 1991]. Such annealing can occur in the shallow subsurface during uplift/burial or glacial sea level and sea bottom-temperature changes [Whiticar *et al.*, 1995] (see below), and at the base of the stability zone the hydrate could be progressively enriched by a

process of continuous melting, upwards transport of gas, and recrystallization at a higher level [see Hyndman *et al.*, 1992, Brown *et al.*, 1996].

Concretions typically exhibit diffusion-limited growth, whereby isolated nuclei deplete the surrounding pore waters of the mineral constituents and this material is replenished through relatively slow diffusive transport [Cody, 1991; Selles-Martinez, 1996]. Norvik and Lekvam [1994] used this model to explain the distribution of hydrate patches growing in submarine sediments, and the same reasoning predicts that large nodules or lenses will be spaced throughout the sediment.

7.4. Thermodynamic Degrees of Freedom and Phase Stability in Porous Media

Incorporating capillary properties into the description of the hydrate system changes how we can apply the Gibbs phase rule as a means of predicting how many phases can coexist in stable equilibrium [Gaydos *et al.*, 1993]. The usual statement of Gibbs phase rule found in textbooks is

$$F = NC - NP + 2 \quad (14)$$

NC is the number of independently acting chemical components, and NP is the number of stable phases. F is the variance or number of degrees of freedom of the system, which is a statement of the number of variables needed to completely define the system minus the number of independent equations that interrelate them. These equations are Gibbs-Duhem equations of the form of (5) written for each of the NP phases. The number 2 refers to the number of non-compositional variables required to describe the state of the system, which for bulk systems are the intrinsic properties of pressure and temperature. If all the chemical and physical variables of the system are specified, there is no variance in the system (this state will be a single point on a phase stability diagram), whereas if one parameter can be varied freely without influencing any others, we have a univariant condition, and so on [Fletcher, 1993].

In capillary systems at thermodynamic equilibrium we note that chemical potentials of individual components must be equal in all phases, and temperature must be uniform across the system, but pressures can change across the curved interfaces between phases. When the configuration of different phases can change freely to adopt a minimum energy condition without mechanical constraint, the Gibbs phase rule becomes

$$F = NC + 1 \quad (15)$$

[e.g., Nitao and Bear, 1996]. For each additional mechanical constraint condition, one of the phase pressures will be eliminated from the total variance [Li and Neumann, 1994]. In a porous medium where water is a completely wetting phase, such a constraint condition applies because the contact angle at the pore wall is fixed at 0° . The fractional proportions of each phase in the porous medium must sum to 1, and only certain configurations of phases in the pore space can satisfy mechanical equilibrium (Figure 10).

While the detailed thermodynamics of capillary systems are beyond the scope of this paper, we can make some useful points. First, the number of phases that can coexist inside a porous medium may differ from that expected for an equivalent bulk system. Second, the mobile phases inside a porous medium will rearrange into a configuration that has a local surface energy minimum; this is not a global free energy minimum. Transitions between stable states may proceed in a discontinuous manner,

with abrupt jumps in saturation and phase pressures [Gaydos *et al.*, 1993; cf. Miller, 1980]. Third, thermodynamic transformations in porous media will exhibit hysteresis. Finally, the thermodynamic state of a phase will depend on its capillary pressure, which is determined by the pore size distribution, surface energy, wettability, phase percentages and, because of hysteresis, the saturation history.

7.5. Elevated BSRs: Inhibition or Disequilibrium?

At ODP sites 889 and 892 the thermal profiles derived from downhole measuring techniques suggested that the temperature at the BSR is too low for it to correspond to the bulk equilibrium position of the methane hydrate-seawater system; that is the BSR is anomalously shallow by a few tens of meters [Whiticar *et al.*, 1996]. However, longer-term measurements reported from the instrumented Hole 892B show that, within error, the position of the regional BSR is in line with the seawater-methane hydrate curve [Davis *et al.*, 1996]. Therefore, the local mismatch of the BSR depth on the vertical seismic profile and sonic logs, with respect to the temperature profile at Site 892, may have been a transient feature associated with drilling disturbance (perhaps either gas migrated upwards or cold drilling water entered the formation).

During ODP Leg 164, thermal profiles through sites on the Blake Outer Ridge revealed an even larger discrepancy in depth to the BSR, which lies 30 to 100 m above the expected position of the base of hydrate stability [Paull *et al.*, 1997; Ruppel, 1997]. These discrepancies are minimum estimates because the pore waters at depth are fresher than seawater, and traces of higher hydrocarbons, CO₂, and hydrogen sulfide may also stabilize the hydrate relative to the pure methane benchmark. It is possible that the displaced BSR on the Blake Ridge is the result of disequilibrium arising from changes in sea level and water temperature since the last glacial maximum [see Westbrook *et al.*, 1994]. Mienert and Posewang [1997] report a second, metastable BSR in an area of slumping on the Norwegian margin that has persisted for thousands of years. However, Ruppel [1997] discounted this possibility as less likely for the Blake area than some kind of inhibition due to the environment within the marine sediments. Most recently, Xu and Ruppel [1999] have argued that the offset in the position of the BSR can be explained as a consequence of upwards flow of fluids and heat. We suggest some possible mechanisms that could displace the BSR even when conditions of quasistatic equilibrium prevail.

The fact that the base of gas hydrate stability should occur at a predictable temperature for a given depth has been used as a way to estimate the heat flow where BSRs are visible on seismic lines [Hyndman *et al.*, 1992]. If the prominent reflector marking the top of free gas is cooler than that predicted by bulk stability conditions, then heat flow values calculated using this assumption will be overestimates.

7.6. Implications for Estimates of Gas Hydrate Volumes

The volume of hydrate present in sediments has been estimated from the degree of freshening as indexed by chloride depletion [Hesse and Harrison, 1981] in pore waters squeezed from sediments recovered from hydrate-bearing intervals. Hydrate volume is calculated from mass balance assuming a starting pore water composition and a likely porosity for the sediment. Our model predicts that hydrate is likely to be concentrated in segregated masses that draw water from the surrounding sediments. In this water depletion scenario the hydrate does not inhabit the original pore space of the sediment,

and the residual pore space is diminished by overconsolidation, so that calculations of the amount of hydrate within a particular depth interval may be underestimates.

Current estimates of gas hydrate volumes made on a more regional scale are based upon values of seismic velocity and reflectivity calculated relative to normally compacting sediments [Lee *et al.*, 1993; Wood *et al.*, 1994; Andreassen *et al.*, 1995]. It is appreciated that such estimates are sensitive to the assumptions made regarding how the hydrate is distributed within the sediment [Dvorkin and Nur, 1993; Anderson, 1994]. Observations from Leg 146 and elsewhere [Ginsburg and Soloviev, 1997] would suggest that the physical properties, and so the seismic response, of sediments adjacent to hydrate concentrations are modified by water depletion. Such overconsolidated sediments will have increased velocity and the reflectivity of interval boundaries will be affected. It is not yet clear whether the mechanisms we invoke for segregated hydrate growth would lead to gas hydrate volumes being underestimated or overestimated, but we caution that the response of the host sediment adds an extra degree of uncertainty to calculations.

8. Summary and Conclusions

We suggest that as a result of capillarity and osmosis, gas hydrate will be distributed heterogeneously in a sequence of sediments according to textural and mineralogical properties. Segregated growth forms are likely in fine sediments, particularly in the near surface and where growth rates are modest. Interstitial hydrate is favored in coarse sediments and may be more prevalent at greater depth, or where the reaction to form hydrate progressed rapidly. Our model is consistent with data available on sediment texture, pore size, and hydrate distribution.

In fine-grained sediments, the hydrate phase may be destabilized thermodynamically, and perhaps inhibited from nucleating, until the prevailing temperature is considerably cooler than the bulk equilibrium value, perhaps by as much as 0.5° to 3°C. This is sufficient to displace the BSR upwards by several tens of meters relative to predictions based on bulk stability equilibrium curves and will increase the depth of first hydrate appearance by a similar amount. These estimates are based on published experimental data and by analogy with ice formation in soils; precise calculations of the capillary effects are given in the companion paper [Henry *et al.*, this issue].

We speculate that where the local influx or in situ production of methane is great, water depletion and strong capillary forces may act to stabilize isolated pockets of free gas well above the normal base of hydrate stability. This may explain occurrences of anomalously low seismic velocity (less than 1.5 km s⁻¹) within the hydrate stability zone at continental margins [Fontana and Mussumeci, 1994; Rowe *et al.*, 1995]. Certain instances of marked seismic attenuation (blanking) that are not accompanied by a commensurate increase in sonic velocity [Wood *et al.*, 1994; W. Wood personal communication, 1998], and so are not easily explicable simply as zones of hydrate precipitation, may also be related to changes in sediment physical properties during water depletion. We suggest that estimates of gas hydrate abundance based upon seismic or other indirect sensing methods should take into account possible host sediment effects.

Notation

| | |
|----------|--|
| <i>g</i> | acceleration due to gravity, m s ⁻² . |
| <i>h</i> | water depth, m. |
| <i>z</i> | depth below sea floor, m. |

| | |
|---------------------|---|
| r_1 | first principal radius of curvature, m. |
| r_2 | second principal radius of curvature, m. |
| r_e | effective, cylindrical-equivalent radius of curvature of pore throat, m. |
| r_t | actual radius of curvature of pore throat, m. |
| r_b | effective radius of curvature of pore body of actual radius r_p , m. |
| r_{nw} | present radius of curvature of pore ice, m. |
| r_{cnt} | minimum radius of curvature to force segregated crystal growth, m. |
| A | surface area, m ² . |
| E_S | cohesive strength of sediment, Pa. |
| K | total surface curvature, m ⁻¹ . |
| K_{AB} | surface curvature of interface between phase A and phase B , m ⁻¹ . |
| K_p | curvature of phase interface inside pore body, m ⁻¹ . |
| K_e | curvature of phase interface entering pore throat, m ⁻¹ . |
| P_A | pressure of phase A , Pa. |
| P_B | pressure of phase B , Pa. |
| $P_{h,seg}$ | phase pressure of hydrate at the critical point of segregation, Pa. |
| P_i | phase pressure of ice, Pa. |
| P_w | phase pressure of (pore)water, Pa. |
| R | gas constant, 8.314 J K ⁻¹ mol ⁻¹ . |
| S^r | solubility of a spherical crystal of radius r , mole fraction. |
| S^0 | solubility of a bulk crystal with effectively zero curvature, mole fraction. |
| $T_{i,bulk}$ | freezing temperature of water to ice under bulk conditions, K. |
| $\Delta T_{i,pore}$ | depression in freezing temperature of ice inside a pore, below bulk freezing temperature, K. |
| V | volume, m ³ . |
| \bar{V}_m | molar volume, m ³ mol ⁻¹ . |
| \bar{V}_i | partial molar volume of component i in a phase, m ³ mol ⁻¹ . |
| γ_{AB} | specific surface energy of interface between A and B phases, J m ⁻² or N m ⁻¹ . |
| γ_{rw} | specific surface energy of ice/water interfaces, J m ⁻² . |
| γ_{mw} | specific surface energy of hydrate/water, J m ⁻² . |
| μ | chemical potential (Gibbs free energy per mole), of a substance, J mol ⁻¹ . |
| μ^0 | chemical potential of a substance in the standard state, J mol ⁻¹ . |
| θ_{iw} | contact angle between ice and water subtended at the grain interface, degrees. |
| ρ_w | specific density of water, kg m ⁻³ . |
| ρ_i | specific density of ice, kg m ⁻³ . |
| σ_0 | overburden stress mobilized in sediment grains, Pa. |
| ΔH_{fi} | specific enthalpy of fusion of ice, J kg ⁻¹ . |

Acknowledgments. We thank Matt Kohn (AE) and two anonymous referees for constructive suggestions. Bruce Yardley gave invaluable help with phase relationships. We are grateful for ideas and comments from Miriam Kastner, Alan Rempel, Bahman Tohidi, David Lysne, Graham Westbrook, Knut Lekvam, Paul Handa, Tim Minshull, Per-Arne Bjørkum, Mark Rodger, and Doug Shearman. Angelo Camerlenghi contributed important observations. Reviews by Ryo Matsumoto and William Bryant improved earlier versions of this manuscript. Olga Zatsepina, Bruce Buffett, Wenye Xu, and Carolyn Ruppel kindly provided preprints. Victor Balachov provided Russian translations. The U.S. Geological Survey supported scientific exchanges. The U.K. Natural Environment Research Council funded M.B.C. through the Rob Kidd Fellowship (Ocean Drilling Program). This paper is dedicated to the memory of Gabriel D. Ginsburg, who inspired and encouraged us.

References

- Adamson, A.W., and A.P. Gast, *Physical Chemistry of Surfaces*, 6th, Ed., 784pp., John Wiley, New York, 1997
- Anderson, A.L., Discussion related to papers by Dillon et al., Brooks et al., and Paull et al., *Ann. N.Y. Acad. Sci.*, 715, 410-411, 1994.
- Andreassen, K., P.E. Hart, P.E. and A. Grantz, Seismic studies of a bottom simulating reflection related to gas hydrate beneath the continental margin of the Beaufort Sea, *J. Geophys. Res.*, 100, 12659-12673, 1995
- Bondarev, E.A., A.G. Groisman, and A.Z. Savvin, Porous medium effect on phase equilibrium of tetrahydrofuran hydrate, paper presented at Second International Conference on Natural Gas Hydrates, United Engineering Foundation, Toulouse, France, June, 2-6, 1996.
- Booth, J. S., M.M. Rowe, and K.M. Fischer, Offshore gas hydrate sample database with an overview and preliminary analysis, *U.S. Geol. Surv. Open File Rep.* 96-272, 28 pp., 1996
- Booth, J. S., W.J. Winters, W.P., Dillon, M.B. Clennell, and M.M. Rowe, Major Occurrences and reservoir concepts of marine clathrate hydrates: Implications of field evidence, in *Gas Hydrates*, edited by J.-P. Henriot and J. Mienert, *Geol. Soc. Spec. Publ.*, 137, 113-128, 1998.
- Borowski, W.S., C.K. Paull, and W. Ussler III, Marine pore-water sulfate profiles indicate in situ methane flux from underlying gas hydrate, *Geology*, 24, 655-658, 1996.
- Brewer, P.G., F.M. Orr Jr., G. Friederich, K.A. Kvenvolden, D.L. Orange, J. McFarlane, and W. Kirkwood, Deep ocean field tests of methane hydrate formation from a remotely operated vehicle, *Geology*, 25, 407-410, 1997.
- Brooks, J.M., A.L. Anderson, R. Sassen, I.R. McDonald, M.C. Kennicutt, and M.L. Guinasso, Hydrate occurrences in shallow subsurface cores from continental slope sediments, *Ann. N. Y. Acad. Sci.*, 715, 381-391, 1994.
- Brown, K.M., N.L. Bangs, P.N. Froelich, and K.A. Kvenvolden, The nature, distribution and origin of gas hydrate in the Chile Triple Junction, *Earth Planet. Sci. Lett.*, 139, 471-483, 1996
- Bruand, A., and R. Prost, Effect of water content on the fabric of a soil material: An experimental approach, *J. Soil Sci.*, 38, 461-472, 1987.
- Carlisle, T.R., The influence of surfaces on natural gas hydrate formation in the rock-sediment environment, paper presented at Fourth International Conference on Water-Rock Interaction, Int. Assoc. Hydrol., Miasa, Japan, Aug. 8-10, 1983.
- Carson, B., G.K. Westbrook, R. Musgrove, and Leg 146 Scientific Party, *Proceedings of the Ocean Drilling Program, Scientific Results*, vol. 146, Ocean Drill. Program, College Station, Tex., 1996.
- Cha, S.B., H. Oaur, T.R. Wildman, and E.D. Sloan, A third-surface effect on hydrate formation, *J. Phys. Chem.*, 92, 6492-6494, 1988.
- Chersky, N.V., and N.E. Mikhailov, Size of equilibrium critical nuclei of gas hydrates (in Russian), *Dokl. Akad. Nauk. SSSR*, 312, 968-971, 1989.
- Churaev, N.V., S.A. Bardasov, and V.D. Sobolev, On the non-freezing water interlayers between ice and a silica surface, *Colloids Surf. A*, 79, 11-24, 1993.
- Claypool, G.E., Influence of water solubility, phase equilibria and capillary pressure on methane occurrence in sediments (abstract), *AAPG Annual Convention, San Diego, Program with Abstracts*, p. A27, Tulsa Oklahoma, 1996.
- Clennell, M.B., M. Hovland, D. Lysne, and J.S. Booth, Role of capillary forces, coupled flows and sediment-water depletion in the habitat of gas hydrate (abstract), *Eos Trans. AGU*, 76 (17), Spring Meet. Suppl., 164-165, 1995.
- Cody, R.D., Organo-crystalline interactions in evaporite systems: The effects of crystallization inhibition, *J. Sediment Petrol.*, 61, 704-718, 1991
- Colbeck, S.C., Configuration of ice in frozen media, *Soil Sci.*, 133, 116-122, 1982.
- Collett, T.S., Natural gas hydrates of the Prudhoe Bay and Kuparuk River area, North Slope, Alaska, *AAPG Bull.*, 77, 793-812, 1993.
- Davis, E.E., K. Becker, K. Wang, and B. Carson, Long-term observations of pressure and temperature in Hole 892B, Cascadia accretionary prism, *Proc. Ocean Drill. Program, Sci. Results*, 146, 299-312, 1996.
- Davis, H. T., *Statistical Mechanics of Phases, Interfaces and Thin Films*, 712 pp., VCH, Berlin, 1996.
- de Lange, G.J., and H.-J. Brumsack, The occurrence of gas hydrate in Eastern Mediterranean mud dome structures as indicated by porewater composition, in *Gas Hydrates*, edited by J.-P. Henriot and J. Mienert, *Geol. Soc. Spec. Publ.*, 137, 167-176, 1998.
- de Roo, J.L., C.J. Peters, R.N. Lichtenthaler, and G.A.M. Diepen,

- Occurrence of methane hydrate in saturated and unsaturated solutions of sodium chloride and water in dependence of temperature and pressure, *AIChE J.*, 29, 651-657, 1983.
- Dholabhai, P.D., P.Englezos, N. Kalogerakis, and P.R. Bishnoi, Equilibrium conditions for methane hydrate formation in aqueous mixed electrolyte solutions, *Can. J. Chem. Eng.*, 69, 800-805, 1991.
- Dickens, G.R., and M.S. Quinby-Hunt, Methane hydrate stability in pore water: A simple theoretical approach for geophysical applications, *J. Geophys. Res.*, 102, 773-783, 1997.
- Dickens, G.R., C.K. Paull, P. Wallace, & ODP Leg 164 Scientific Party, Direct measurement of in situ methane quantities in a large gas hydrate reservoir, *Nature*, 385, 426-428, 1997.
- Dillon, W.P., M.W. Lee, K. Fehhhaber, and D.F. Coleman, Gas hydrates on the Atlantic continental margin of the United States: Controls on concentration, in *The Future of Energy Gases*, edited by D.G. Howell, *U.S. Geol. Surv. Prof. Pap.*, 1570, 330-347, 1993.
- Dvorkin, J., and A. Nur, Rock physics for characterization of gas hydrates, in *The Future of Energy Gases*, edited by D.G. Howell, *U.S. Geol. Surv. Prof. Pap.*, 1570, 293-298, 1993.
- Englezos, P., and S. Hall, Phase equilibrium data on carbon dioxide hydrate in the presence of electrolytes, water soluble polymers and montmorillonite, *Can. J. Chem. Eng.*, 72, 887-893, 1994.
- Ershov, E.D., Y.P. Lebdenko, E.M. Chuvilin, and V.S. Yakushev, Peculiarities of gas hydrate formation in sands, Paper presented at 6th International Conference on Permafrost, Am. Soc. Civ. Engrg., Fairbanks, Alaska, Jun. 6-11, 1993.
- Everett, D.H., The thermodynamics of frost damage to porous solids, *Trans. Faraday Soc.*, 57, 1541-1551, 1961.
- Fletcher, P., *Chemical Thermodynamics For Earth Scientists*, 464pp, Longman Sci. and Tech., London, 1993.
- Fontana, R.L., and A. Musumeci, Hydrates offshore Brazil, in *Natural Gas Hydrates*, edited by E.D. Sloan Jr., J. Happel and M.A. Hnatow, 106-113, N. Y. Acad. Sci., New York, 1994.
- Gaydos, J., D. Li, and A.W. Neumann, Implications of the phase rule for capillary systems containing surfaces and three-phase contact lines with surface and linear constraint relations, *Colloids Polym. Sci.* 271, 715-725, 1993.
- Ginsburg, G.D., Gas hydrate accumulation in deep-water marine sediments, in *Gas Hydrates*, edited by J.-P. Henriot and J. Mienert, *Geol. Soc. Spec. Publ.*, 137, 51-62, 1998.
- Ginsburg, G.D., and V.A. Soloviev, Mud volcano gas hydrates in the Caspian Sea, *Bull. Geol. Soc. Den.*, 41, p 95-100, 1994.
- Ginsburg, G.D., and V.A. Soloviev, Methane migration within the submarine gas-hydrate stability zone under deep-water conditions. *Mar. Geol.*, 137, 49-57, 1997.
- Ginsburg, G.D., and Soloviev, V., *Submarine Gas Hydrates*, 216 pp., VNIIOkeangeologia / Norma, St. Petersburg, Russia, 1998.
- Ginsburg, G.D., V.A. Soloviev, R.E. Cranston, T.D. Lorenson, and K.A. Kvenvolden, Gas hydrates from the continental slope, offshore Sakhalin Island, Okhotsk Sea, *Geo Mar. Lett.*, 13, 41-48, 1993.
- Griffiths, F.J., and R.C. Joshi, Change in pore-size distribution due to consolidation of clays, *Geotechnique*, 39, 159-167, 1989.
- Gunnink, B.W., and J. El-Jayyousi, Soil-fabric measurement using phase-transition porosimetry, *J. Geotech. Eng.*, 119, 1019-1036, 1993.
- Handa, Y.P., Effect of hydrostatic pressure and salinity on the stability of gas hydrates, *J. Phys. Chem.*, 94, 2652-2657, 1990.
- Handa, Y.P., and D. Stupin, Thermodynamic properties and dissociation characteristics of methane and propane hydrates in 70-Å-radius silica-gel pores, *J. Phys. Chem.*, 96, 8599-8603, 1992.
- Henry, P., M. Thomas, and M.B. Clennell, Formation of natural gas hydrates in marine sediments, 2. Thermodynamic calculations of stability conditions in porous sediments, *J. Geophys. Res.*, this issue.
- Hesse, R., and W.E. Harrison, Gas hydrates (clathrates) causing pore-water freshening and oxygen isotope fractionation in deep water sedimentary sections of terrigenous continental margins, *Earth Planet. Sci. Lett.*, 55, 603-613, 1981.
- Higskole, B., A.R. Nerheim, T.M. Svarts, and E.J. Samuelsen, Laser light scattering studies of gas hydrate formation kinetics, in *Proceedings, 4th International Offshore and Polar Engineering Conference*, pp. 323-327, ISOPE, Osaka, Japan, 1994.
- Hovland, M., D. Lysne, and M.J. Whitticar, Gas hydrate and sediment gas composition, ODP Hole 892A, *Proc. Ocean Drill. Program, Sci. Results*, 146, 151-162, 1996.
- Hovland, M., J.W. Gallagher, M.B. Clennell, and K. Lekvam, Gas hydrates and free gas volumes in marine sediments: Example from the Niger Delta front, *Mar. Pet. Geol.*, 14, 245-255, 1997.
- Hyndman, R.D., and E.E. Davis, A mechanism for the formation of methane hydrate and seafloor bottom-simulating reflectors by vertical fluid expulsion, *J. Geophys. Res.*, 97, 7025-7041, 1992.
- Hyndman, R.D. and G.D. Spence, A seismic study of methane hydrate bottom simulating reflectors, *J. Geophys. Res.*, 97, 6683-6698, 1992.
- Hyndman, R.D., J.P. Foucher, M. Yamano, A. Fisher, and Scientific Team of Ocean Drilling Program Leg 131, Deep sea bottom-simulating reflectors: Calibration of the base of the hydrate stability field as used for heat flow estimates, *Earth Planet. Sci. Lett.*, 109, 289-301, 1992.
- Iversen, N., and B.B. Jorgensen, Diffusion coefficients of sulfate and methane in marine sediments, *Geochim. Cosmochim. Acta*, 57, 571-578, 1993.
- Jallut, C., J. Lenoir, C. Bardot, and C. Eyraud, Thermoporometry: Modeling and simulation of a mesoporous solid, *J. Membrane Sci.*, 68, 271-282, 1992.
- Kamath, J., and R.E. Boyer, Critical gas saturation and supersaturation in low-permeability rocks, *SPE Form. Eval.*, SPE 25563, 247-253, 1995.
- Kastner, M., An inclusion hourglass pattern in synthetic gypsum, *Am. Mineral.*, 55, 2128-2130, 1970.
- Kastner, M., K.A. Kvenvolden, M.J. Whitticar, A. Camerlenghi, and T.D. Lorenson, Relation between pore fluid chemistry and gas hydrates associated with bottom-simulating reflectors at the Cascadia Margin, Sites 889 and 892, *Proc. Ocean Drill. Program, Sci. Results*, 146, 175-189, 1996.
- Kimura, K., Silver, E., Blum, P. and Leg 170 Scientific Party, *Proceedings of the Ocean Drilling Program, Initial Reports*, vol. 170, Ocean Drill. Program, College Station, Tex., 1998.
- Konrad, J.C., and C. Duquenois, A model for water transport and ice lensing in freezing soils, *Water Resour. Res.*, 29, 3019-3024, 1993.
- Kraemer, L.M., R.M. Owen, and G.R. Dickens, Lithology of the upper gas hydrate zone at Hole 994C, Blake Outer Ridge (abstract), *Eos Trans. AGU*, 78(46), Fall Meet. Suppl., F344, 1997.
- Kvenvolden, K.A., Gas hydrates: Geological perspective and global change, *Rev. Geophys.*, 31, 173-187, 1993.
- Kvenvolden, K.A., G.D. Ginsburg, and V.A. Soloviev, Worldwide distribution of subaquatic gas hydrates, *Geo Mar. Lett.*, 13, 32-40, 1993.
- Lee, M.W., D.R. Hutchinson, W.P. Dillon, J.J. Miller, W.F. Agena, and B.A. Swift, Method of estimating the amount of in-situ gas hydrates in deep marine sediments, *Mar. Pet. Geol.*, 10, 493-506, 1993.
- Lekvam, K., and P. Ruoff, A reaction-kinetic mechanism for methane hydrate formation in liquid water, *J. Am. Chem. Soc.*, 115, 8565-8569, 1993.
- Li, D., and A.W. Neumann, Phase rule for capillary systems, *Adv. Colloid Interface Sci.*, 49, 147-195, 1994.
- Lowell, S., and J.E. Shields, *Powder Surface Area and Porosity*, 250 pp., Chapman and Hall, New York, 1991.
- MacDonald, I.R., N.L. Guinasso, Jr., R. Sassen, J.M. Brooks, and L. Lee, Gas hydrate that breaches the sea floor on the continental slope of the Gulf of Mexico, *Geology*, 22, 699-702, 1994.
- Machel, H.G., and E.A. Burton, Burial-diagenetic sabkha-like gypsum and anhydrite nodules, *J. Sediment. Petrol.*, 61, 394-405, 1991.
- MacKay, M.E., R.D. Jarrard, G.K. Westbrook, R.D. Hyndman, and Shipboard Scientific Party of ODP Leg 146, Origin of bottom-simulating reflectors: Geophysical evidence from the Cascadia accretionary prism, *Geology*, 22, 459-462, 1994.
- Makogon, Y.F., *Hydrates of Natural Gas*, 237 pp. Penwell, Tulsa, Okla., 1981.
- Makogon, Y.F., Gas hydrate formation in porous medium, paper presented at Second International Conference on Natural Gas Hydrates, United Engineering Foundation, Toulouse, France, June 2-6, 1996.
- Malone, R.D., *Gas hydrates, Top. Rep. DOE/METC/SP-218*, U.S. Dep. of Energy, Washington, D.C., 1985.
- Mashirov, S.G., D.Y. Stupin, G.D. Ginsburg, and V.A. Soloviev, Simulation experiment in hydrate formation from aqueous solution (in Russian), *Dokl. Akad. Nauk. SSSR*, 316, 205-207, 1991.
- Melnikov, V., and A. Nesterov, Hydrate formation from gas solutions in water (in Russian), *Dokl. Akad. Nauk. SSSR*, 333, 495-497, 1993.
- Melnikov, V., and A. Nesterov, Modelling of gas hydrates formation in porous media, Second International Conference on Natural Gas Hydrates, United Engineering Foundation, Toulouse, France, June 2-6, 1996.
- Mienert, J., and J. Posewang, Flach- und Tiefwassergashydrate in Sedimenten polarer Kontinentalränder des Nordatlantiks: Geophysikalische Signature der Instabilität, *Geowissenschaften*, 15, 287-292, 1997.

- Miller, J.J., M.W. Lee, and R. von Heune, An analysis of a seismic reflection from the base of a gas hydrate zone, offshore Peru, *AAPG Bull.*, 75, 910-924, 1991.
- Miller, R.D., Freezing phenomena in soils, in *Introduction to Soil Physics*, edited by D. Hillel, pp. 254-299, Academic, San Diego, Calif., 1980.
- Mitchell, J.K., *Fundamentals of Soil Behavior*, 2nd ed., 504 pp., John Wiley, New York, 1993.
- Nitao, J.J., and J. Bear, Potentials and their role in transport in porous media, *Water Resour. Res.*, 32, 225-250, 1996
- Norvik, H., and K. Lekvam, Mass- and heat transfer effects on gas hydrate growth, in *Proceedings, 4th International Offshore and Polar Engineering Conference*, pp. 329-332, ISOPE, Osaka, Japan, 1994.
- Oaur, H., S.B. Cha, T.R. Wildeman, and E.D. Sloan, The formation of natural gas hydrates in water-based drilling muds, *Trans Inst Chem. Eng.*, 70A, 48-54, 1993.
- Paull, C.K., R. Matsumoto, P. Wallace, and Leg 164 Scientific Party, *Proceedings of the Ocean Drilling Program, Initial Reports*, vol. 164, Ocean Drill. Program, College Station, Tex., 1997.
- Paull, C.K., W. Ussler III, and W.S. Borowski, Sources of methane to form marine gas hydrates, *Ann. N. Y. Acad. Sci.*, 715, 392-409, 1994.
- Pearson, C., Physical properties of natural gas hydrate deposits inferred by analogy with permafrost (abstract), *Eos Trans. AGU*, 62, (45), 953, 1981.
- Pearson, C.F., P.L. Halleck, P.L. McGuire, R. Hermes, and M. Mathews, Natural gas hydrates: A review of in situ properties, *J. Phys. Chem.*, 87, 4180-4185, 1983.
- Pecher, I., C.R. Ranero, R. von Heune, T. Minshull, and S.C. Singh, The nature and distribution of bottom simulating reflectors at the Costa Rica convergent margin, *Geophys. J. Int.*, 133, 219-229, 1998.
- Peyrt, T.M., F. Orti, and L. Rosell, Sulfate platform-basin transition of the lower Werra Anhydrite (Zechstein, Upper Permian), western Poland: Facies and petrography, *J. Sediment. Petrol.*, 63, 646-658, 1993.
- Putnis, A., M. Prieto, and L. Fernandez-Diaz, Fluid supersaturation and crystallization in porous media, *Geol. Mag.*, 132, 1-13, 1995.
- Rempel, A.W., and B.A. Buffett, Formation and accumulation of gas hydrate in porous media, *J. Geophys. Res.*, 102, 10151-10164, 1997.
- Rempel, A.W., and B.A. Buffett, Mathematical models of gas hydrate accumulation, in *Gas Hydrates*, edited by J.-P. Henriot and J. Mienert, *Geol. Soc. Spec. Publ.* 137, 63-74, 1998.
- Rodger, P.M., T.R. Forester, and W. Smith, Simulations of the methane hydrate / methane gas interface near hydrate forming conditions, *J. Fluid Phase Equilibria*, 116, 326-332, 1996.
- Rowe, M.M., Fischer, K.M., Gettrust, J.F. and Booth, J.S., Geophysical evidence for pathways of gas escape from submarine gas hydrates (abstract), *Eos Trans. AGU*, 76 (17), Spring Meet Suppl., 163, 1995.
- Ruppel, C., Anomalously cold temperatures observed at the base of the gas hydrate stability zone on the U.S. Atlantic passive margin, *Geology*, 25, 699-702, 1997.
- Scherer, G.W., Freezing gels, *J. Non Crystalline Solids*, 155, 1-25, 1993.
- Selles-Martinez, J., Concretion morphology, classification and genesis, *Earth Sci. Rev.*, 41, 177-210, 1996.
- Shearman, D.J., Displacement of sand grains in sandy gypsum crystals, *Geol. Mag.*, 118, 303-306, 1981.
- Shipley, T.H., M.H. Houston, R.T. Buffler, F.J. Shaub, K.J. McMillen, J.W. Ladd, and J.L. Worzel, Seismic evidence for widespread possible gas hydrate horizons on continental slopes and rises, *AAPG Bull.*, 63, 2204-2213, 1979.
- Singh, S.C., T.A. Minshull, and G. Spence, Velocity structure of a gas hydrate reflector, *Science*, 260, 204-206, 1993.
- Sloan, E.D., *Clathrate Hydrates of Natural Gases*, 641 pp., Marcel Dekker, New York, 1990.
- Smelik, E.A., and H.E. King, Crystal growth studies of natural gas clathrate hydrates using a pressurized optical cell, *Am. Mineral.*, 82, 88-98, 1997.
- Stoll, R.D., J. Ewing, and G.M. Bryan, Anomalous wave velocities in sediments containing hydrates, *J. Geophys. Res.*, 76, 2090-2094, 1971.
- Tardy, Y., and A. Novikoff, Activité de l'eau et déplacement des équilibres gibbsite-kaolinite dans les profils latéritiques, *C. R. Acad. Sci., Ser. II*, 306, 39-44, 1988.
- Tessier, D., A. Lajudie, and J.-C. Petit, Relation between the macroscopic behavior of clays and their microstructural properties, *Appl. Geochem., Suppl. Issue 1*, 151-161, 1992.
- Tissot, B.P., and D.H. Welte, *Petroleum Formation and Occurrence*, 538 pp., Springer-Verlag, New York, 1978.
- Tohidi, B., A. Danesh, and A.C. Todd, Modeling single and mixed electrolyte-solutions and its applications to gas hydrates, *Chem. Eng. Res. Des.*, 73, 464-472, 1995.
- Tohidi, B., Danesh, A. and Todd, A.C., On the mechanism of gas hydrate formation in subsea sediments, *Abstr. Pap. Am. Chem. Soc.*, 213, 37-39, 1997.
- Tréhu, A.M., G. Lin, E. Maxwell, and C.A. Goldfinger, Seismic reflection profile across the Cascadia subduction zone offshore central Oregon: New constraints on methane distribution and crustal structure, *J. Geophys. Res.*, 100, 15101-15116, 1995.
- Trofimuk, A.A., N.V. Cherskiy, Y.F. Makogon, and V.P. Tsarev, Possible mechanisms of accumulation of natural gas, in *International Geological Review 1968-1981, API Reprint Ser.*, vol. 6, pp. 72-76, Am. Pet. Inst., Tulsa, Okla., 1972.
- Ussler, W. III, and C.K. Paull, Effects of ion exclusion and isotopic fractionation on pore water geochemistry during gas hydrate formation and decomposition, *Geo Mar. Lett.*, 15, 37-44, 1995.
- Waseda, A., Organic carbon content, bacterial methanogenesis, and accumulation of gas hydrates in marine sediments, *Geochem. J.*, 32, 143-157, 1998.
- Westbrook, G.K., B. Carson, R.J. Musgrave and Leg 146 Scientific Party, *Proceedings, Ocean Drilling Program, Initial Reports*, vol. 146, Ocean Drill. Program., College Station, Tex., 1994.
- Whiticar, M.J., Hovland, M., Kastner, M. and Sample, J.C., Organic geochemistry of gases, fluids and hydrates at the Cascadia accretionary margin, *Proc. Ocean Drill. Program, Sci. Results*, 146, 385-398, 1996.
- Williams, P.J., and M.W. Smith, *The Frozen Earth*, 303 pp., Cambridge Univ. Press, New York, 1991.
- Wood, W.T., P.L. Stoffa, and T.H. Shipley, Quantitative detection of methane hydrate through high-resolution seismic velocity analysis, *J. Geophys. Res.*, 99, 9681-9695, 1994.
- Xu, W., and C. Ruppel, Predicting the occurrence, distribution, and evolution of methane gas hydrate in porous marine sediments, *J. Geophys. Res.*, 104, 5081-5095, 1999.
- Yardley, B.W.D., On some quartz-plagioclase veins in the Connemara schists, Ireland, *Geol. Mag.*, 112, 183-190, 1975.
- Yousif, M.H., and E.D. Sloan, Experimental investigation of hydrate formation and dissociation in consolidated porous media, *SPE Reservoir Eng.* 6, 452-458, 1991.
- Zakrewski, M., and Y.P. Handa, Thermodynamic properties of ice and of tetrahydrofuran hydrate in confined geometries, *J. Chem. Thermodyn.*, 25, 631-637, 1993.
- Zatsepina, O.Y., and B.A. Buffett, Thermodynamic conditions for the stability of gas hydrate in the seafloor, *J. Geophys. Res.*, 103, 24127-24139, 1998.
- Zharikov, V.A., Fluids in geological processes, in *Fluids in The Crust*, edited by K.I. Schmulovich, B.W.D. Yardley, and G.G. Gonchar, pp. 203-273, Chapman and Hall, New York, 1994.

J.S. Booth and W.J. Winters, United States Geological Survey, Woods Hole, Mass. 02543-1598. (jbooth@usgs.gov; bwinters@usgs.gov)

M.B. Clennell, Centro de Pesquisa em Geofísica e Geologia, Universidade Federal da Bahia, Rua Caetano Moura 123, Salvador, 40210-340 Brazil. (clennell@cpgg.ufba.br)

P. Henry, Laboratoire de Géologie de l'Ecole Normale Supérieure, 24 rue Lhmond, 75231 Paris 5, France. (henry@opale.ens.fr)

M. Hovland, Statoil, N-4035, Stavanger, Norway. (MHOVLAND@statoil.com)

(Received May 22, 1998; revised April 12, 1999; accepted April 21, 1999.)